AALBORG UNIVERSITET

COMPARING SIMULATED OUTDOOR TAG YIELDS OF *CHLOROCOCCUM LITTORALE*:

WILDTYPE VERSUS IMPROVED SORTED POPULATION

Hanna Böpple

M.Sc.-Thesis

School of Engineering and Science

Title:	**Comparing simulated outdoor TAG yields of *Chlorococcum littorale*: wildtype versus improved population**
Student:	**Hanna Böpple (hboepp14@student.aau.dk) 20141331**
Study program:	**M.Sc. Sustainable Biotechnology**
Semester:	**3.+4. Semester**
Project period:	**1/9/2015-10/6/2016**
ECTS:	**60**
Supervisors:	**Iago D. Teles (AP) (Iago.DominguezTeles@WUR.nl)** **Dorinde Kleinegris (AP)** **Peter Westermann (AAU)**
Number of pages:	**48**
Appendix:	**13**

_____

Hanna Böpple

I hereby declare that the work submitted is my own work. I understand that plagiarism is defined as presenting someone else's work as one's own without crediting the original source. I am aware that plagiarism is a serious offense, and that anyone committing it is liable to academic sanctions.

Acknowledgements

I spent the last 10 month working towards my Masters degree, and was able to include a very exciting stay at AlgaePARC. I would like to thank my supervisors Peter Westermann and Dorinde Kleinegris, who helped me to overcome the bureaucratic obstacles and made this internship possible in the first place. I enjoyed the 4 month I´ve spent in Wageningen a lot, thanks to the great people (in AP!) that made me feel very welcomed there and helped out with all kind of practical issues.

My greatest thanks goes to Iago. You were creating a spot for me there in AlgaePARC and supported me in all matters from day 1 (and before...). Beside the excellent project supervision, not only during my stay, but throughout the whole period afterwards until now, you were always available for a great laugh, motivational talks in seemingly desperate situations and "quick" Skype chats at all times and situations. Together we mastered (almost) all modelling obstacles, something I couldn´t have thought of just a year ago.

A final thanks goes to my friends, family and especially my boyfriend, supporting me in all matters even while being far away for most of the time.

Abstract

This project focused on understanding and exploiting the lipid dynamics of *Chlorococcum littorale*, a marine microalgae species. Microalgae are presented as a suitable source of oils for the commodities market, however, current cost analyses makes it imperative to increase productivities and to reduce costs to achieve an economically feasible production. A sorted population of *C. littorale*, namely S5, showed a 1.9-fold triacylglycerol (TAG) productivity under continuous light conditions in a previous work. This thesis compared productivities of biomass and its components of *C. littorale* wildtype and S5 under simulated Dutch summer conditions. The indoor experiments with controlled day/night cycles were operated in a 1.9 L flat panel photobioreactor as a batch nitrogen runout. The final total biomass concentration in S5 was almost doubled when compared to Wt (Wt: 4.65 g/L, S5: 8.51 g/L) and TAG concentration increased 2.5-fold (Wt: 0.98 g/L, S5: 2.49 g/L). These first results confirmed the potential of S5 for microalgae production.

The second part of this thesis dealt with using the above mentioned experiments for establishing input parameters to estimate productivities under different light scenarios with a model in MATLAB. A mechanistic model (previously developed for *Scenedesmus obliquus*), describes biomass production and, under N-starvation, carbon partitioning between starch and TAG accumulation. The experiments above mentioned were used to validate the model for both *C. littorale* strains. The model was furthermore used to compare the outdoor simulations with experiments actually carried out outdoors, as a result it was possible to use the model for productivity simulations under different locations (Wageningen, the Netherlands; Oslo, Norway; Rio de Janeiro, Brazil; Cádiz, Spain).

Model simulations on the indoor experiments followed experimental measurements for biomass growth and composition, whereas the TAG concentration of S5 was underestimated (with an accordingly underestimated total biomass). The model applied on the outdoor experiment showed a good fit, where only the last day of total biomass was underestimated. The comparison of the location simulations resulted in a clear assumption of a decreased photosynthetic efficiency at high light intensities, hence increasing light intensities were not resulting in proportionally increasing productivities as light saturation occurs.

Contents

List of acronyms

CHO	Total carbohydrates without starch
CI	Confidence interval
DW	Dryweight (g/L)
e.g.	*exempli gratia*; for example
EtOH	Ethanol
FACS	Fluorescence-activated cell sorting
FAME	Fatty Acid Methyl Esters
GC	Gas chromatography
GOPOD	glucose oxidase/peroxidase; Megazyme Glucose Determination Reagent
i.e.	*id est*; that is to say
M+M	Material and Methods
ms	Model parameter for maintenance requirements
N	Nitrogen
N+	Nitrogen replete phase
N-	Nitrogen deplete phase
N=0	Timepoint at nitrogen depletion
OD	Optical density (nm)
PBR	Photobioreactor
PUFA	Polyunsaturated fatty acid
STA	Starch (model parameter)
t	Time
TAG	Triacylglycerol
p.	Page
ph	Photons
Wt	Wildtype

List of figures

List of tables

1. Introduction

With a declining availability of feasible lands and shrinking natural resources, particularly crude oil reserves, a discussion around the necessity towards sustainable development of energy and fossil based products is redundant. Population growth and an ongoing climate change are not to be prevented, but rather the adaptation of technologies and lifestyles may decide over a succeeding continuity on earth.

Biotechnological research over the years established many technologies which are applied in various industrial fields. Bioplastics, enzyme production as well as high-value products in cosmetics or pharmaceutical industry are examples for a successful shift from petro- and chemical production processes towards a sustainable bioeconomy (Wijffels & Barbosa, 2010).

When it comes to alternative fuel sources, biodiesel research is going through an onward development of technologies, though always accompanied by a constant food versus fuel discussion. Based on vegetable oils or residual fats from animal production, most production plants of biodiesel commonly utilize soybeans. Due to the decreasing availability of arable lands, the yields of those energy crops are not high enough to support a worldwide replacement of fossil fuels through biodiesel (Scarlat, Dallemand, & Pinilla, 2008). Extensive soy plantations (not only for biofuels, but moreover as a high-protein feed for livestock) endanger biological diversity through deforestation and competition as a food and feed source, hence adding more pressure to the topic (Reinhardt, Rettenmaier, & Köppen, 2008). In other words, biodiesel research is aiming for decreased environmental impacts while sustaining to be comparable in performance and economically competitive. Comparing oil productivities (t/ha/year) of the two major oil crops (rapeseed : 1.4 t/ha/y; soybean: 0.5 t/ha/y) with the potential oil production from oleaginous algae (*Chlorella vulgaris*: 7.2 t/ha/y; *Nannochloropsis*: 20-30 t/ha/z), it becomes clear why research contemplates the utilization of microalgae for commercial purposes (Scott et al., 2010). Several hundred microalgae strains are known to have potential higher lipid productivities (per ground area) and higher growth rates than land crops (Bowles, 2007; Qiang Hu et al., 2008). The utilization of marine microalgae species would be an enormous advantage when considering lack of arable land, as production is not depended on fresh water sources or soil qualities. The pilot facility of the Sahara Forest Project[1] is just one example of marine algae making the desert a suitable production location.

[1] located in Jordan, combines seawater cooled greenhouses, solar power, algae cultivation (and more) to revegetate desert lands and provide fresh water, food, renewable energy; http://saharaforestproject.com/algae

Microalgae are considered to provide third-generation biofuels, whereas the storage lipid triacylglycerol (TAG) was found to be the best lipid for biodiesel production (Srivastava & Prasad, 2000). TAGs represent 20–50 % of the cells dry weight and are mainly accumulated during the stationary phase under stress conditions (Qiang Hu et al., 2008). Converting triacylglycerols to biodiesel is alike to the conversion of TAGs from oleaginous land crops, using transeserification, whereat the fatty acid esters serve as biodiesel.

A sustainable production does not only focus on environmental and social aspects but as well on economic feasibility. In this regard biofuels from microalgae became rather uncompetitive due to average market prices and production costs of petroleum based products. The ongoing oil crisis (since 2014) makes the need for improvements in microalgae-based technology urgent. Essential for commercial production is the combination with production of bulk chemicals, e.g. food and feed ingredients for achieving competitive prices in the commodities market. Besides technical improvements regarding cultivation, cell harvest and downstream processes, an increased productivity through strain improvement could make microalgae-based products more competitive, where the main focus has to be on maximizing the lipid content of algal cells (Wijffels & Barbosa, 2010). Firstly the strain improvements should increase the overall productivity, as the total lipid yield depend on both lipid content and areal productivity (Mata, Martins, & Caetano, 2010). In addition to an improved general productivity, research on mechanisms behind lipid accumulation are giving way for metabolic engineering. Previous works on engineered starchless mutants have shown a successful increase of the TAG productivity (de Jaeger et al., 2014; Li et al., 2010; Ramazanov & Ramazanov, 2006).

General problems in biorefining microalgae are presented by the separation technologies for the different cell constituents as harsh disruption methods have to break up the thick cell wall and centrifugation is only viable with higher biomass concentrations than 3 g/L (Draaisma et al., 2013). A suitable algae strain should therefore be able to be grown under high cell densities to increase the amount of total biomass and improve the productivities (Q. Hu, Kurano, Kawachi, Iwasaki, & Miyachi, 1998; Tredici, 2010).

As light is the substrate of an phototrophically grown algal cell, screening of algae focuses on the ability to grow under low light levels, as well as being able to withstand high light intensities, while keeping a high photosynthetic efficiency (Beckmann et al., 2009; Durnford & Falkowski, 1997). Decreasing photosynthesis efficiencies are a common difficulty especially during summertime at lower latitudes, as light saturation occurs at higher irradiances (Tredici, 2010). Previous works tried to solve those problems with the introduction of smaller antenna sizes, which allowed the algae to grow at high irradiances and thereby doubled the photosynthetic activity (Polle, Benemann, Tanaka, & Melis, 2000).

Modelling is a good alternative to explore all above mentioned limitations and bottlenecks of microalgae-based technology (Bernard, 2011). Models can be used to evaluate scenarios and the effect of isolated variables on demonstration scale microalgae production. Since microalgae technology is still in its infancy, the lack of available large scale data could be solved using a modelling approach (Csögör, Herrenbauer, Perner, Schmidt, & Posten, 1999; Kirschbaum, Küppers, Schneider, Giersch, & Noe, 1998). Models need to be, however, validated for each strain, due to specific biological necessities. A few models have been developed for microalgae, mostly describing growth as dependent on light (Baquerisse, Nouals, Isambert, dos Santos, & Durand, 1999; Slegers, Lösing, Wijffels, van Straten, & van Boxtel, 2013; Slegers, van Beveren, Wijffels, van Straten, & van Boxtel, 2013). The limitation of growth models is that they do not describe the dynamics of intracellular components under stress conditions. Since it is known that microalgae accumulate storage compounds under nitrogen-starvation (as the example of the current research), a model is required that describes the carbon partitioning after N-starvation (i.e. the fate of the photons inside the cells). There are some models to describe lipids production by microalgae, but mostly oversimplifying the energy from photosynthesis, or simulating only TAG accumulation without considering interconversion rates between intracellular biomass components (Kliphuis et al., 2012; Klok et al., 2013). The carbon partitioning has been described and modelled by Breuer and co-authors, for the green microalgae *Scenedesmus obliquus* under continuous light (both Wt and a starchless mutant) (Breuer, Lamers, Janssen, Wijffels, & Martens, 2015). In such model, the dynamics between starch and TAG accumulation are described under N-starvation, giving a potent tool to estimate the productivity of both components under different scenarios. To run reliable models, however, biological parameters from each species are necessary, hence experiments should be run to provide such input parameters, prior to the modelling work (Benvenuti et al., 2016; Breuer et al., 2015). The focus of the current thesis is therefore, to estimate the input parameters for *Chlorococcum littorale* (both Wt and an improved strain), to simulate production under simulated outdoors conditions.

The choice for *C. littorale* was based on screening experiments of Benvenuti et al. (2014), which compared TAG content, biomass productivity and photosynthetic efficiency in a nitrogen runout batch using 9 different strains. A disadvantage arising from the method of a nitrogen stressed cultivation, which is triggering higher TAG contents, is a decreased biomass productivity in some microalgae. The green microalgae *Chlorococcum littorale* however sustained its photosynthetic activity during nitrogen depletion, leading to a 3-fold increase in of lipid concentration. Hence *C. littorale* was considered a suitable candidate for cultivation focused on a high TAG production (Benvenuti, Bosma, Cuaresma, et al., 2015; Chihara, Nakayama, Inouye, & Kodama, 1994).

1.1. Previous experiments

The current work is under the umbrella of the AlgaePARC[2] project, which has the general goal to increase lipid productivity of microalgae for commercial applications. Experiments were performed, prior to this thesis project, with *Chlorococcum littorale* to understand the biology related to both growth and lipid accumulation (Benvenuti, Bosma, Cuaresma, et al., 2015; Cabanelas, van der Zwart, Kleinegris, Barbosa, & Wijffels, 2015).

Previous experiments on *C. littorale* wildtype were carried out to estimate the biological parameters necessary as input for the mechanistic model (see workflow Fig. 1) under both indoor and outdoor summer conditions. This thesis went further with the application of the mechanistic model to estimate the productivities under different climates.

The experimental part of this thesis was done using a new improved strain of *Chlorococcum littorale*, namely S5. This strain was developed (prior to this work) using the approach presented by Cabanelas et al. (2015). In summary: the S5 strain was developed via cell sorting, used to establish new cell populations with increased TAG productivity. The details on how S5 was established were submitted as a research paper.

[2] **AlgaePARC** (**Algae P**roduction **A**nd Research **C**entre) at Wageningen UR, http://www.algaeparc.com

1.2. Aim

The general aim of this thesis was to estimate productivities of biomass and its constituents of *Chlorococcum littorale* under outdoor conditions.

A pre-existing mechanistic model was validated to estimate the productivities of *Chlorococcum littorale* Wt under simulated Dutch summer conditions. The same model was also validated as well for simulations of an improved strain of *C. littorale* (S5) and its productivities under simulated summer conditions. Finally, biomass and its constituents productivities were estimated under different geographic locations for both strains of *Chlorococcum littorale*.

The work flow presented in Figure 1 was designed to achieve the aim of this work. Indoor experiments under simulated Dutch summer conditions were carried out with both Wt and S5 strains of *Chlorococcum littorale*. The biological parameters derived from the indoor experiments were used to validate the mechanistic model that describes the productivity of biomass and biomass constituents of *Scenedesmus obliquus* (Breuer et al., 2015). Outdoor experiments were carried out with the Wt strain and used to calibrate the model under Dutch summer conditions. Finally, the model was used to simulate and compare productivities of both strains under different climates (Wageningen, the Netherlands; Oslo, Norway; Cádiz, Spain; and Rio de Janeiro, Brazil).

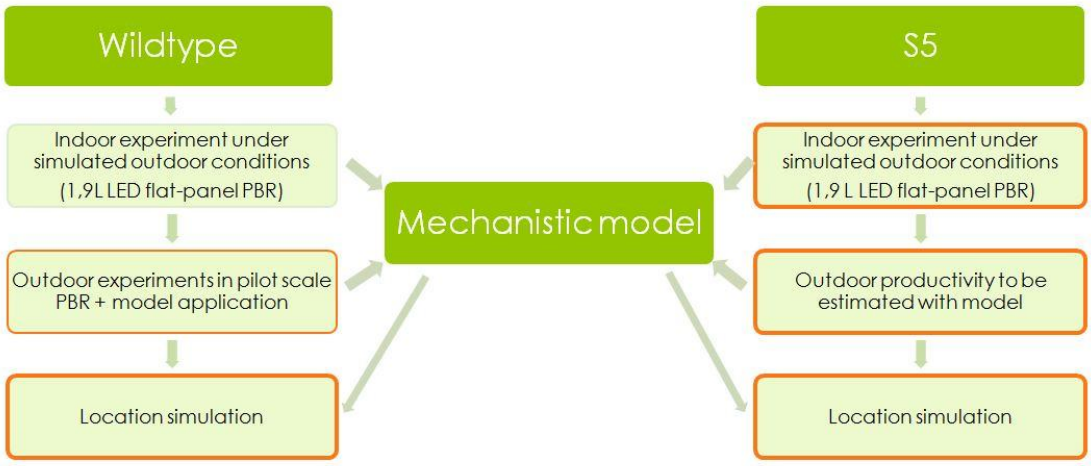

Figure 1: Project overview; experiments outlined in orange have been performed for this thesis project, other data were supplied from a previous work within the framework of the same project (see 1.1)

2. Theoretical background

2.1. *Chlorococcum littorale*

The unicellular marine microalgae *Chlorococcum littorale* (Chlorococcales, Chlorophyta) was first isolated from a saline pond near the coast of Japan in 1990 and is described by Chihara et al. (1994).

During growth cells have a spheroidal diameter ranging from 5 µm to 8 µm. An increased diameter of up to 11 µm is observed during stationary phase, while under stress conditions the diameter increases up to 14 µm. Cell walls consist of several layers, are relatively thin (<0.5 µm) and thicken with age. The nucleus of the vegetative cells is located in the anterior part of the cells. Each cell contains a single chloroplast which again contains a conspicuous pyrenoid. The pyrenoid matrix is covered with two starch sheets, starch grains can as well accumulate between the chloroplasts lamellae. Lipid globules vary in size, generally many globules can be found in the cytoplasm of the vegetative cells as well as in the cytoplasm of the zoospores (Chihara et al., 1994).

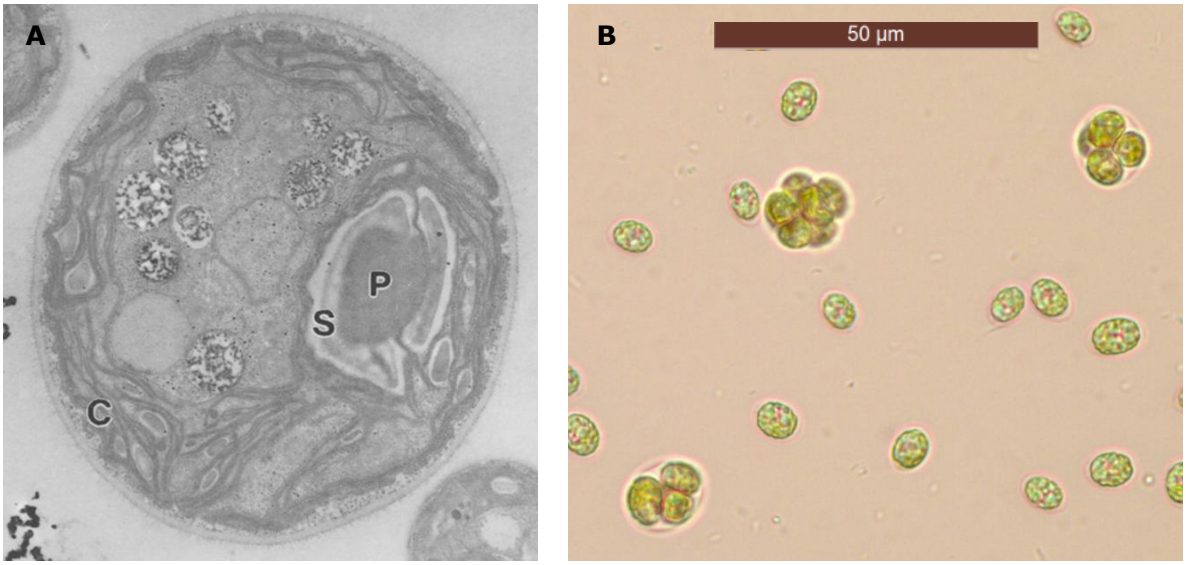

Figure 2: A: Electron microscopic image of a vegetative cell of *Chlorococcum littorale,* showing the chloroplast (C) and the pyrenoid matrix (P) which is surrounded by a starch sheath (S), by M. Chihara (1994); B: Bright field microscopiv image of *C. littorale* S5 during growth phase (magnification of 400x)

The optimal growth temperature is reported between 15 °C and 28 °C, with a lethal maximum of 30 °C. The alga cannot be cultivated at a pH below 3 and shows a good growth at pH levels above 4. As a marine algae, *Chlorococcum littorale* is dependent on salinity during cultivation. A salt content of 1.5 % NaCl resulted in the best growth within the tested range from 1.5-9.0 % NaCl (Chihara et al., 1994).

A specific quality of *C. littorale* is the exceeding tolerance of up to 60 % CO_2. However, CO_2 contents over 30 % yielded in significant lower biomass rates, while maximal output

rates were obtained within a CO_2 content of 5-20 % (Chihara et al., 1994; Q. Hu et al., 1998). Investigations on the optimal cell density under various light intensities showed a sustained biomass growth under a light intensity up to 2000 µmol/m²/s (Q. Hu et al., 1998).

C. littorale is reported to reach a total lipid content of 10-15 % (g/g DW) under nitrogen replete conditions (Q. Hu et al., 1998). The total lipid content consists of polar membrane lipids (in steady amounts related to the total biomass) and storage lipids in the form of triacylglycerides (TAGs), which can be accumulated as lipid bodies in the cells. TAG-productivity can be triggered through nitrogen-starvation, reaching an increased total lipid content of up to 35 % (g/g DW) during continuous lightning (Benvenuti, Bosma, Cuaresma, et al., 2015; Chihara et al., 1994). Due to its high capacity of lipid accumulation in combination with sustained photosynthetic activity under nitrogen-starvation, *C. littorale* seems to be a promising strain for TAG production.

2.2. Triacylglycerol

The lipid class of triacylglycerols (TAGs) is represented in most of the plant and animal fats and oils that are available on the market. TAGs are esters[3] formed by glycerol and three fatty acid chains. Fatty acid (FA) chains range usually from 10-20 carbon atoms in length and both saturated and unsaturated forms are found in plants and as body fat in humans and animals. Double bounds in unsaturated FA make the molecule more soluble and decrease the melting temperature. Long chain poly unsaturated fatty acids (LC-PUFA; C_{20}-C_{24}) are not naturally found in animal tissue and are known for their positive impact on the cardio vascular systems when ingested (Harris, Kris-Etherton, & Harris, 2008). One of the most known class of PUFA has its first double bond on the third carbon atom, classified as a omega-3-fatty-acid and a potential high-value product in the market of food supplements. Any FA that cannot be synthesized by animals on their own is called an essential fatty acid.

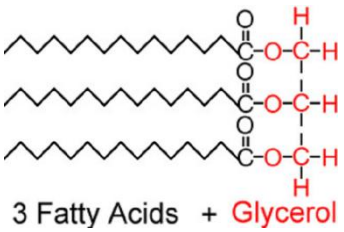

Figure 3: Scheme of a triacylglycerol with three similar fatty acids, saturated as no double bounds between the carbon atoms are present.

[3] FA reacts with alcohol group of the glycerol to form water and the ester

Most of the eukaryotic microalgae naturally accumulate fatty acids in form of triacylglycerols under stress conditions (Breuer, Lamers, Martens, Draaisma, & Wijffels, 2012; Stephenson, Dennis, Howe, Scott, & Smith, 2010). The oil content of oleaginous microalgae can accumulate up to 50-70 % (of DW), mostly stored in form of TAGs (Chisti, 2008; Qiang Hu et al., 2008).

There are numerous combinations of TAGs, depending on the number of carbon atoms of each fatty acid chain, defining a specific fatty-acid profile. Most algae species form primarily FA chains between 16 to 18 carbons in length, similarly to higher plants (Ohlrogge & Browse, 1995). On the other hand microalgae show a greater variation in FA composition than land crops and are generally rich in polyunsaturated FA (Qiang Hu et al., 2008). The essential fatty acid linoleate (C_{18}) is commonly found in microalgal oils, besides being present in vegetable oils from corn, rape seed, sunflower and soybean, and thereby showing a clear potential for industrial use (Draaisma et al., 2013). Long chain poly unsaturated fatty acids are not naturally found in animal tissue and are known for their positive impact on the cardio vascular systems when ingested (Harris et al., 2008), thus being of big interest as potential high-value products. Eicosapentaenoic acid (EPA, 20:5) and docosahexaenoic acid (DHA, 22:6) are the two best known omega-3-FA and are primarily found in oily fish (e.g. mackerel or salmon). Ongoing exploitation of fish-stocks and accumulating pollutants in the fish oil is leading the expanding market to its limits and alternative solutions are required in near future (Tonon, Harvey, Larson, & Graham, 2002). Several experiments on marine microalgae showed high levels of PUFAs, including EPA and DHA and production for commercial applications is an approaching goal (Grima et al., 1995; Tonon et al., 2002; Vazhappilly & Chen, 1998).

Besides the utilization for food and feed, microalgal TAGs are considered for potential industrial utilization as biofuels. After extraction and purification of algal oils, a transesterification[4] of TAGs with (mainly) methanol to the corresponding fatty acid methyl esters takes place (production can also be done with ethanol, generating the equivalent ethyl esters). The residual glycerol can be used in pharmaceutical- or food industries. Economical aspects of microalgal biodiesel production have to be improved substantially, even though production is already industrially available to some extent. Oleaginous microalgae has to be inexpensively produced in large quantities, before becoming competitive to low-value products (e.g. fossil fuels) or high-value products (e.g. food supplements) on the commodities market (Chisti, 2008).

[4] Transesterification reacts 3 mol of alcohol for each mole of TAG to produce 1 mol of glycerol and 3 mol of methyl esters. In industrial processes 6 mol of methanol for each TAG is used to direct the reaction towards biodiesel (Fukuda, Kondo, & Noda, 2001)

2.3. Nitrogen run-out batch cultivation in flat panel PBR

Already since the first experiments from Spoehr & Milner (1949), it was discovered that the cultivation of microalgae under stress conditions (e.g. nutrient limitation or high light intensities) is leading to an enhanced lipid accumulation and maximum lipid contents of up to 70-80 % (of DW) have been reported (Qiang Hu, 2004; Roessler, 1990). To such purpose nitrogen limitation/starvation is the most common and effective strategy to increase lipid accumulation in microalgae (Rodolfi et al., 2009). However, a main detriment caused under nitrogen starvation is often a general reduction of photosynthetic activity (Berges, Charlebois, Mauzerall, & Falkowski, 1996; Parkhill, Maillet, & Cullen, 2001). The main impact on metabolic mechanisms due to the nitrogen starvation is made on the photosystem II and its light utilization (Berges et al., 1996). Through the absence of extracellular nitrogen, the synthesis of PSII proteins is substantially reduced and the amount of cellular pigmentation decreased (Geider, La Roche, Greene, & Olaizola Miguel, 1993; Pruvost, Van Vooren, Cogne, & Legrand, 2009; Solovchenko et al., 2013). Light absorption is therefore reduced, which can be directly measured as the (light) absorption coefficient (see M+M, 3.4). A general indication for photosynthetic activity of healthy microalgal cells is the quantum yield of PS II (Fv/Fm, see 3.4), with values between 0.6 and 0.7, lower values are expressing abiotic or biotic stress (e.g. through N-starvation) (Young & Beardall, 2003).

Benvenuti et al. (2014) compared different green microalgae species in terms of TAG production during nitrogen depletion and found out that *Chlorococcum littorale* almost doubled the fatty acid productivity in the N-starvation phase in comparison with a N-replete culture (time-average fatty acid production from 78 mg/L/d (N+) to 126 mg/L/d (N-)). The experiment showed that the decrease of photosynthetic activity during nitrogen depletion is smaller than in other species, leaving *C. littorale* with a higher TAG content. In summary, nitrogen starvation is a promising method for enhancing lipid production in *C. littorale*. The green algae sustains its photosynthetic activity during nitrogen depletion, leading to a 3-fold increase of lipid concentration (Benvenuti, Bosma, Cuaresma, et al., 2015; Chihara et al., 1994).

2.4. Model description

A mechanistic model was developed for *Scenedesmus obliquus* under continuous light by Breuer et al. (2015). The model simulates algae growth, thus functional biomass production. Functional biomass (X) is describing total biomass until nitrogen depletion, including biomass constituents as starch, TAGs and carbohydrates, as well as proteins, genetic material and ashes. The model simulates a nitrogen run-out batch, which means

that all nitrogen will be consumed before other nutrients, starting a starvation phase. The accumulation of carbon compounds and conversions of other biomass constituents are described during starvation and the model can therefore be used to predict the TAG productivity of *C. littorale*.

The model is based on the photosynthetic carbon partitioning of green microalgae, i.e. the fate of the photosynthetically converted photon energy into the cell. Two scenarios are distinguished, cultivation under nitrogen replete conditions (N+) and nitrogen depletion (N-). After covering the maintenance requirements (ms), the photosynthetic energy is either lead to build functional biomass solely (while N+) or split between synthesis of carbohydrate, starch and TAG (during N-starvation). This partitioning can be calculated specifically for the algae strains (wildtype and S5, in the current research), describing biomass growth (q_{ph}, ms, absorption coefficient), nitrogen concentration, initial biomass constitution (starch, other carbohydrates than starch, TAG and functional biomass), light scenario (light intensity and duration) and partitioning between starch and TAG (pA, pB).

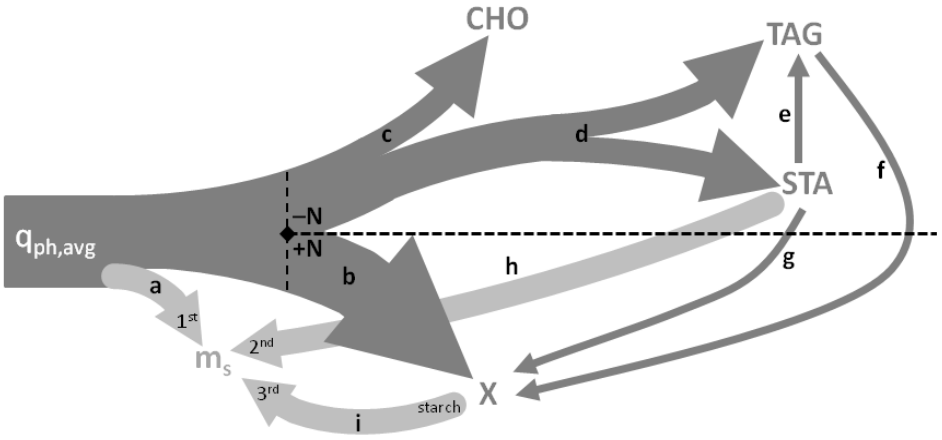

Figure 4: Scheme of partitioning of photosynthetic energy depending on extracellular nitrogen presence: N-replete (N+) and N-deplete (N-). Maintenance requirements (ms) during light periods are firstly covered by the energy of absorbed photons (a). In dark respiration ms energy is covered by starch (STA) degradation (h). If there is no accumulated STA available, ms will be covered from the starch fraction of the functional biomass X (i). During N-depletion, accumulation of carbohydrates other then starch (CHO), TAG and STA (d) takes place (from Wieneke, 2015)

During nitrogen replete phase functional biomass is produced exclusively (no synthesis of CHO, TAG and starch) (b). After nitrogen depletion the general carbohydrate (other than starch) levels are kept constant (c), and the residual energy is partitioned between TAG and starch (d). The proportion between TAG and starch synthesis is specific for each scenario and defined through the estimated parameters pA and pB (see detailed model description, Appendix, p. 55). Starch to TAG degradation (e) is possible under certain conditions (see model description, Appendix p. 62)

MathWorks® MATLAB (version R2015b) was used to perform the model simulations.

3. Material and Methods

3.1. Preculture

A preculture was grown in shake flasks to inoculate the photobioreactors with the necessary initial biomass concentration of ~80 g/L. A duplicate of sterile 250 ml Erlenmeyer flasks, containing 50 ml algae culture were inoculated from an agar plate containing the *C. littorale* strains (the agar plates were prepared using the same cultivation medium with the addition of 12 g/L agar). Cultivation was carried out in an Infors Multitron Shaker incubator (HT, Netherlands) with 60 µmol/m²/s continuous lightning (TL-D Reflex 36 W/840, Philips, Netherlands), 120 rpm and temperature at 25° C. The algae culture was refreshed after 7 days with the addition of 50 ml medium. Optical density was measured regularly. This procedure was done similarly for both Wt and S5 strains of *C. littorale*.

3.2. Reactor set-up

The indoor experiments were conducted in two flat panel airlift-loop photobioreactors (Figure 4); the Infors Labfors 5 Lux (1.8 L working volume, 0.08 m² surface area, 20.7 mm light path) with 260 warm white LEDs (approx. 4000 K, spectral distribution see Appendix p. 52).

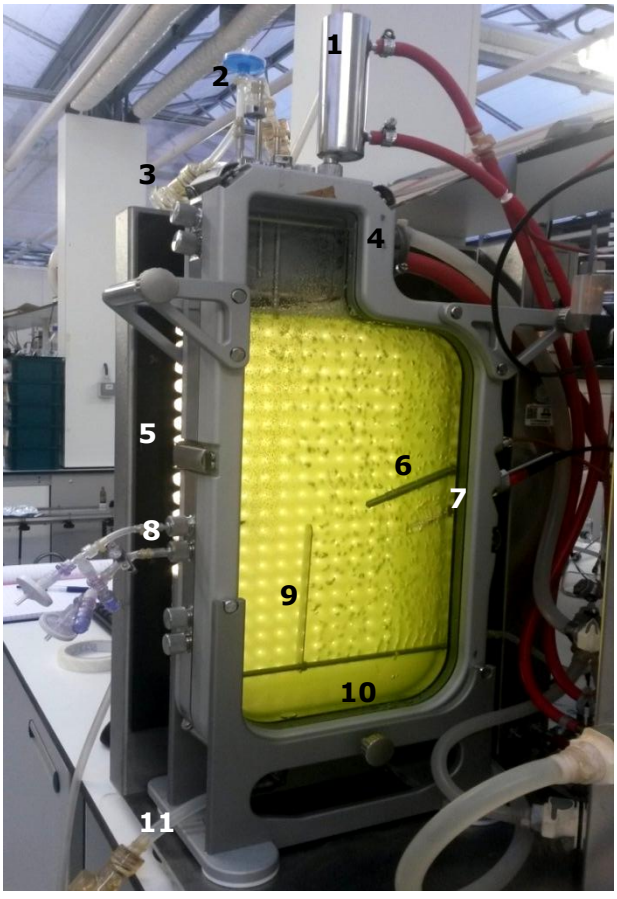

Figure 5: Infors Labfors 5 including light panel, adjacent water chamber for temperature control and culture vessel (1.9 L). Light shield plates are not shown, but covered permanently the whole glass surface (of culture chamber) during cultivation.

1 Condenser
2 Pressure release/Overflow
3 Inoculation port
4 Water chamber outlet/overflow
5 Irradiation unit with 260 LEDs
6 Temperature sensor
7 pH sensor
8 Sampling ports (two)
9 Flow deflector (baffle)
10 Air pipe (sparger)
11 Harvest valve/Drain

An airflow of 2 L/min through the perforated spargertube on one side of the baffle provides mixing through an airlift-loop.

The Infors Labfors 5 was equipped with a touch control panel wherefrom light intensity, temperature, pH, CO_2 and airflow were regulated and monitored. The temperature was regulated through the adjacent water chamber and set to constant 25 °C. The pH was automatically regulated to 7±0.1 via CO_2 addition (maximum of 2 %) in the airflow. 15 ml of 2 % antifoam solution were added within the first three cultivation days, to avoid a loss of culture volume through foam overflowing.

The media contained natural, filtered (0.2 µm) saltwater (from Zeeland, the Netherlands) and a nitrogen free stock solution (see Table 1) as nitrogen runout batches were performed. The initial nitrogen concentration of 125 mg/L (as 10.7 mM KNO_3) was added prior to inoculation via the inoculation port.

Table 1: Composition of the N-free stock solution to be added to enrich the sea water. Concentrations in medium are referent to the addition of 10 ml/L of sea water. pH was adjusted to 7.5-7.6 with NaOH prior to use.

N-free stock	Conc. in Medium	per liter substrate
KH_2PO_4	1.7 mM	11.5 g
Na_2EDTA	173 µM	3 g
Trace mineral stock (Tab. 2)		50 ml
Deionised H_2O until		1000 ml

Table 2: Composition of the trace mineral solution to be added to the solution in table 1. The trace minerals solution not clear, hence, pH needs to be adjusted to 4with NaOH to dissolveeverything.

Trace mineral stock	Conc. in Medium	per liter substrate
$Na_2EDTA*H_2O$	282 µM	45 g
$FeSO_4$, 7 H_2O	108 µM	30 g
$MnCl_2$, 2H_20	11 µM	1.71 g
$ZnSO_4$, 7 H_20	2.3 µM	0.66 g
$Co(NO_3)_2$, 6 H_20	0.24 µM	70 mg
$CuSO_4$, 5 H_20	0.1 µM	24 mg
Na_2MoO_4,2H_20	1.1 µM	242 mg

3.2.1. Light supply

Light intensity was calibrated to a maximum of 1500 µmol/m²/s in both reactors. A Dutch summer day was simulated with 16 hours of sinusoidal light intensity, followed by 8 hours darkness during the night period (Eq. 1).

$$I(t) = \left(\frac{t}{16h} * \pi\right) * 1500 \frac{\mu mol}{m^2 * s} \qquad \text{Eq. 1}$$

As biomass samples during the night were necessary for the modelling part, the day/night cycles were inverted due to practical reasons. To avoid the influence of external light sources, both reactors were covered with light shield plates at all time. Figure 6 shows the applied light supply as well as the daily sampling points.

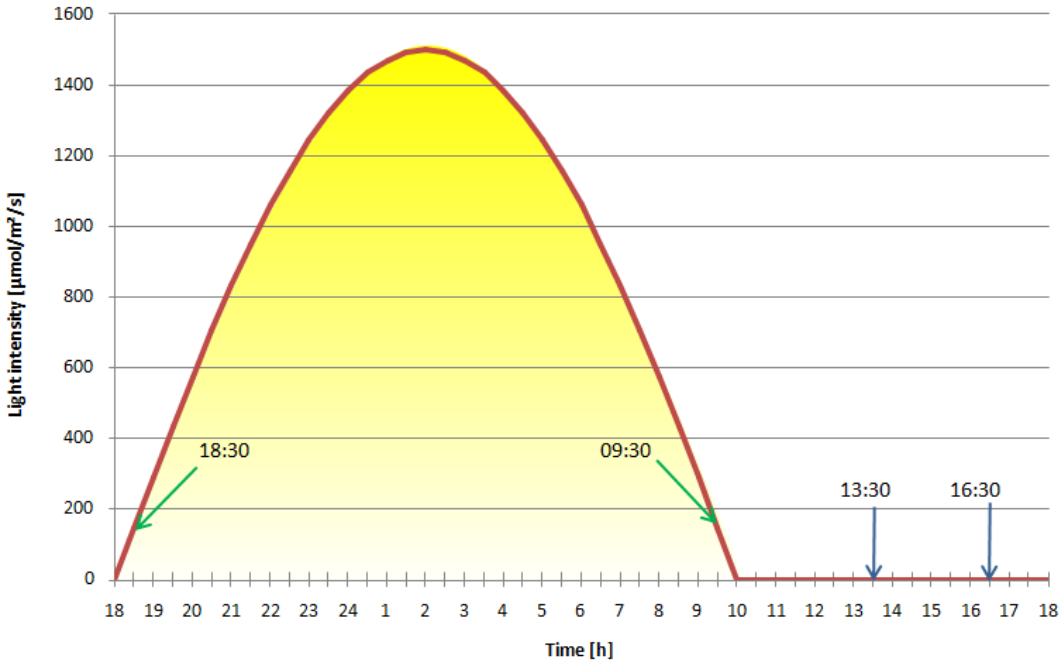

Figure 6: Sampling scheme applied on experiments with a simulated sinus-shaped Dutch summer irradiation. The solar noon at 1500 µmol/m²/s is reached after 8 h (exactly half the daylight period). One light period lasted for 16 h, followed by 8 h of darkness. Samples were taken right after sunrise, before sunset and twice during the night, which is why the day/night cycle was inverted (so dark samples could be taken in the afternoon)

3.3. Outdoor experiment

The outdoor experiment with *C. littorale* wildtype was performed in a 90 L horizontal tubular reactor system (Fig. 7) similarly as described by (Benvenuti, Bosma, Klok, et al., 2015). The system was inoculated to reach an initial biomass concentration of 0.6 g/L in N-free natural seawater (same media composition as in 3.2., sterilization was done by addition of 5 ppm hypochlorite).

The pilot run was performed in August 2015 with a cultivation duration of 11 days. Biomass analysis were conducted similarly as the indoor experiments (see 3.4). The sampling scheme was similar to what is depicted at Figure 6. Samples were taken right after sunrise (06:30) and before sunset (21:00). One sample in the middle of the day was taken at 14:00, to follow up the production of storage compounds. The difference between sunset to sunrise samples could estimate night biomass losses (NBL), while the biochemical composition of such samples could indicate which components were respired during the night to cover maintenance.

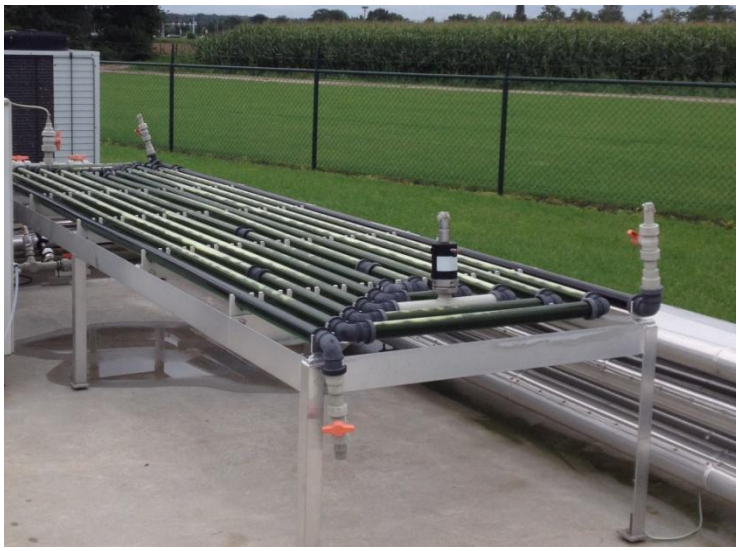

Figure 7: Horizontal tubular outdoor PBR in which the outdoor experiment was performed. Reactor volume: 90 L, ground area: 4.6 m², 0.05m distance between tubes.

3.4. Biomass analysis

Daily measurements

As shown in Fig. 6, 4 daily samples were taken, at sunrise and sunset, as well as two night samples, 3 and 6 hours prior sunrise. Each of the taken samples were immediately analysed with the following measurements below and biomass samples were frozen and freeze-dried for 24 h and stored at -20 °C for later analyzes (total carbohydrates, starch, fatty acids).

OD

The optical density of the algal culture was measured in a spectrophotometer (HACH, DR5000) at wavelengths of 680 nm and 750 nm immediately after sampling. The samples were diluted to an OD ranging between 0.2-0.8 to be within the detection limits required for OD and QY measurements. While the OD_{680} was mainly used as an indication for the culture vitality (chlorophyll fluorescence peak around 680 nm), the cell concentration was reflected by the OD value at wavelength 750 nm.

Dryweight

Culture samples were filtered in Whatman® glass microfiber filters (Ø55 mm, pore size 0.7 µm, Whatman International Ltd, Maidstone, UK). The filters were prewashed, dried (24 h, 105 °C) and weighed. Filters with samples were washed two times with 20 ml MiliQ water, dried again and kept in a desicator (> 2 h, room temperature) prior to weighing. The biomass concentration was expressed in g/L.

Quantum Yield (QY)

The photosystem II activity of the cells was determined through a QY measurement with a fluorometer (AquaPen-C AP-C 100, Photon System Instruments, Czech Republic). Where the maximum quantum yield (Fv/Fm) is expressed by the ratio between emitted and absorbed photons of the cells (Eq. 2). The minimum level of fluorescence of dark-acclimated cells after exposure to a non-actinic beam is measured as F_0. While the maximum fluorescence (F_m) is measured after a strong actinic light pulse (Benvenuti, Bosma, Cuaresma, et al., 2015; Warner, Lesser, & Ralph, 2010).

$$\mathrm{Fv/Fm} = \frac{\mathrm{Fm} - \mathrm{F0}}{\mathrm{Fm}} \qquad \text{Eq. 2}$$

2 ml diluted algae sample (OD_{750} between 0.2 - 0.8) in a 4 ml cuvette were kept 10 min in the dark prior measurement.

Absorbance coefficient

The absorbance spectrum was determined by a fibre optic spectrometer (AvaSpec-2048, Avantes BV, Apeldoorn, Netherlands; light source: AvaLight-Hal) according to the manufacturers protocol. The measurement was including the spectrum from 400 nm to 800 nm. Light scattering was corrected by a subtraction of the average absorption (abs_λ) between 740 nm and 750 nm.

$$a_{rep} = \frac{\sum_{400}^{700} abs_\lambda \frac{\ln(10)}{z}}{300 \cdot c_{DW}} \qquad \text{Eq. 3}$$

with z: light path of the precision cell
c_{DW}: dry weight concentration in the cell

Dissolved and intracellular nitrogen concentration

1 ml algae suspension was centrifuged for 5 minutes at 13300 rpm (Micro Star 17R, VWR®) and the supernatant kept cool (4-8 °C). The dissolved, extracellular nitrogen concentration was measured with a nutrient analyzer (AQ2, SEAL Analytical Inc., USA) according to the NO3 method by SEAL-Analytical.

The intracellular nitrogen concentration was determined from two chosen freezedried biomass samples (inoculation and beginning of N-depletion). Biomass samples were also

analyzed for the composition in N via combustion followed by chromatography (Flash EA 2000 elemental analyser, ThermoFisher Scientific , USA)

Carbohydrates

The amount of total carbohydrates were measured in technical triplicates. 1 mg of freezedried biomass was weighed into bead-beating tubes (Lysing Matrix D, MP Biomedicals, France) and 1 ml of MilliQ water added. After 3 cycles with 60 sec in a bead-beater (4000 rpm, 60 sec pause; Precellys®24, Bertin Technologies, France), 50 µl supernatant were transferred into a fresh glass tube. 0.5 ml 5 % phenol were added, 2.5 ml concentrated sulphuric acid were given directly on the surface and the samples left for incubation at room temperature for 30 min. Finally the closed tubes were vortexed and their optical density measured with a spectrophotometer (HACH, DR5000) at a wavelength of 483 nm.

The final carbohydrate content was calculated from a glucose calibration range (g/L: 0.1; 0.08; 0.06; 0.04; 0.02; 0.02; 0), which was freshly prepared with every batch of analyzed samples. Two positive controls with 1 mg of starch were included, moisture content and the difference in molar weights between glucose and starch were comprised.

Starch

As the mechanistic model includes the generation and degeneration of Starch, the total carbohydrate content alone was not sufficient enough for a detailed conversion model. Sample were measured in technical duplicates and a D-glucose positive control was included.

The starch analysis is an adaptation of the enzymatic method of Fernandes et al. (2011); using a starch assay kit (Megazyme K-TSTA 07/11, Ireland) for hydrolyzing starch into glucose and quantify the glucose content.

10 mg of freeze dried biomass were dissolved in 1 ml 80% (v/v) ethanol (EtOH) and disrupted during 3 cycles bead beating (4000 rpm, 60 sec break; Precellys®24, Bertin Technologies, France; Lysing Matrix E, MP Biomedicals, France). Biomass including beads were transferred into fresh glass tubes and the bead tubes rinsed 4 times with 80 % (v/v) EtOH. After mixing on a vortex, the samples were incubated for 5 min in a 80-85 °C waterbath. Another 5 ml of 80 % EtOH were added to the samples prior mixing and centrifuging for 5 min at 2500 rpm (1580R, LABOGENE). Once the biomass was disrupted and the starch precipitated, the supernatant was discarded and a hydrolysis of starch to glucose was performed with a starch assay kit (Megazyme K-TSTA 07/11, Ireland). The remaining steps were carried out corresponding to the Megazyme kit protocol. Absorbance was measured spectrophotometrically (HACH,DR5000) at a wavelength of 510 nm where the reagent blank consisted of 0.1 ml Mili-Q and 3 ml

GOPOD reagent. 0.1 ml glucose standard solution and 3 ml GOPOD reagent were included as a positive control. A calibration line was established out of following D-glucose concentrations; g/L: 1; 0.8; 0.6; 0.4; 0.2; 0.

Fatty acids (TAG/PL)

Lipid extraction, separation into triacylglyceride and polar acyl lipids and quantification were performed as described by Breuer et al. (2013). Briefly, cells were mechanically disrupted in a solution of chloroform/methanol, two internal standards (C:15; C:19) were added and all acyl lipids are separated by a solvent based extraction. After a transesterification of the fatty acids to fatty acid methyl esters (FAMEs), a GC/MS column chromatography is used for quantification and identification of the detected FAMEs.

3.5. Calculations

The specific growth rate (Eq. 4) was calculated as the change in biomass concentration (expressed as natural logarithm) as a function of time from inoculation until nitrogen starvation.

$$\mu = \frac{\ln(DW_{N=0} - DW_{t_0})}{t_{N=0} - t_0} \qquad \text{Eq. 4}$$

with DW: dry weight of biomass (g/L)
t=0: cultivation start
N=0: timepoint of N-starvation

Biomass productivity (Eq. 5) during growth phase was calculated as the change in biomass concentration (g/L) between inoculation and nitrogen starvation.

$$P_{cx} = \frac{DW_{N=0} - DW_{t_0}}{t_{N=0} - t_0} \qquad \text{Eq. 5}$$

with DW: dry weight of biomass (g/L)
t=0: cultivation start
N=0: timepoint of N-starvation

Biomass yields (g/ mol photon) on light were calculated by division of the biomass productivity (Eq.5) by the corresponding total amount of light impinging on the reactor surface (Infors: 4.4 mol/m²/d, outdoor experiment and different locations see 3.7).

Night Biomass Loss (NBL) was calculated as the difference of measured dryweight (g/L) before and after the night (in %), averaged over the nitrogen depleted cultivation period.

The average TAG productivity (Eq. 6) was calculated as the change in TAG concentration (g/L) for the total N-starvation period.

$$P_{TAG,avg} = \frac{TAG_f - TAG_{N=0}}{t_f - t_{N=0}} \quad \text{Eq. 6}$$

with TAG: TAG concentration (g/L)
N=0: start of N-starvation
t=f: timepoint of N-starvation

The maximum average TAG productivity ($P_{TAG,max}$, g/L/d) was calculated according to Eq. 6, with the exception that only the period from N-starvation (N=0) to the highest TAG productivity was accounted (Wt:t=0-24 h; S5: t=0-72 h; Outdoor: t=0-24 h)

TAG yields (g/ mol photon) on light were calculated by division of the TAG productivity ($P_{TAG,avg}$ or $P_{TAG,max}$ respectively) by the corresponding total amount of light impinging on the reactor surface (Infors: 4.4 mol/m²/d, outdoor experiment and different locations see 3.7).

3.6. Data analyses

The sample standard deviation (SD) was calculated between the biological replicates for every estimated model parameter. The estimated SDs were used to show the data variability between biological replicates for productivities and kinetic parameters (Table 4). The standard deviations were also used to estimate the 95% confidence intervals (with a two-tailed T-distribution) for every experimentally estimated parameter used to run model simulations (Appendix, Table 6). These calculations were carried out with Microsoft Excel 2010.

The confidence intervals (as stated above) were used to evaluate goodness of fit between experimentally measured values and simulated values. As a result, the dot plots between experimentally measured values and simulated values show the upper and lower confidence intervals (Appendix, Fig. 21, 22).

3.7.Outdoor climate data

In the second part of this thesis the model is used to estimate algae production of *C. littorale* under different climates. In addition to the base-case Wageningen (the Netherlands), locations with different day lengths and different maximal light intensities were chosen. Temperature was not included in the simulations (and hence not

important for the choice of location), as both indoor and outdoor systems are temperature controlled.

Four different locations were chosen to simulate production potential of both *C. littorale* Wt and S5. Several structural conditions have to be complied of a location to serve as a suitable production site. Obvious factors as day length and solar irradiation are measurable criteria which have the most influence on cultivation. Furthermore the location should have close access to seawater (in Wageningen it is solved through storage tanks and road transport from the coast of Zeeland, the Netherlands). An efficient regional infrastructure has to be given for mastering the logistics (e.g. sewage system, transports, availability of chemicals and equipment etc.).

Light scenarios for Wageningen, Oslo (Norway), Rio de Janeiro (Brasil) and Cádiz (south of Spain) are shown in Fig. 8. The location of Oslo was chosen to investigate the effect of a longer day length with decreased light intensities (due to higher latitude). Rio and Cádiz have similar daylight periods while Cádiz shows significant higher light intensities. Cultivation periods from April to August for Wageningen and Oslo were assumed while Rio and Cádiz were assumed to be cultivated all year round. Input parameters (day length, light intensity) are derived from the average of all months during this period.

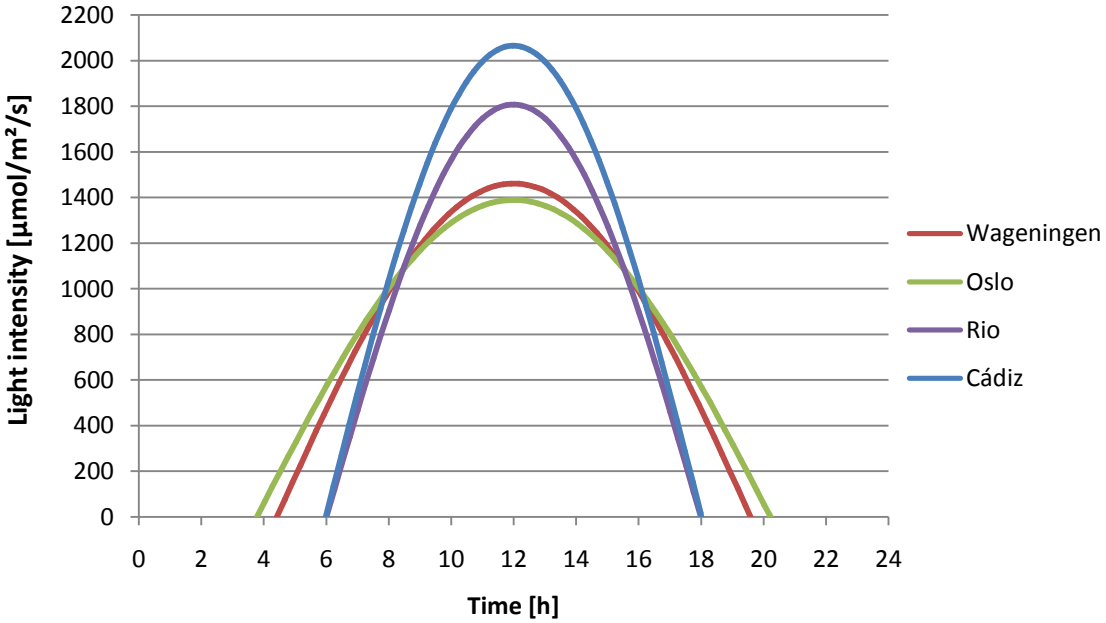

Figure 8: Schematic sinus-shaped daily irradiation for Wageningen, Oslo, Rio de Janeiro and Cádiz. Each line is derived from real local measurements (as explained at 3.7, materials and methods) and were used to calculate the average daily amount of light to be used for the medolling. Average daily amount of light is dependent on both maximum light intensity and day length.

The mechanistic model by G. Breuer assumes a steady light intensity over the whole period of cultivation. Therefore the average photosynthetically active radiation (PAR) over

the day was calculated and incorporated as a light block during daytime (see detailed model description, Appendix p. 52).

The parameter of light intensity (I) that is used for modelling was derived by integrating the light-sinus of the indoor experiments. When it comes to the outdoor cultivation, an averaged light value for a sinus-shaped curve would lead to a significant overestimation of the total amount of light because cloud coverage, shading, or a blurry atmosphere caused by mist or dust throughout the day would be completely neglected. Therefore the total daily amount of light outdoors was calculated and expressed as the "average daily light integral" (DLI [mol/m²/day]) from solar radiation data for each location (Table 3) .

Table 3: Light supply for the simulated locations of Wageningen, Oslo, Rio and Cádiz. The average daily light integral (DLI) is based on the (model) parameters day length (dlds) and light intensity (I0). Averages for Wageningen and Oslo are calculated from April-August, while a whole year average is shown for Rio de Janeiro and Cádiz.

	Unit	Wageningen	Oslo	Rio	Cádiz
Daylength	h	15.2	16.4	12.0	12.0
DLI	mol/m²/d	33.1	31.5	37.8	41.8
Light intensity	µmol/m²/s	606	532	876	966

The used solar radiation data was derived from the HelioClim radiation Databases of SoDa[5], which is estimating total solar irradiance and irradiation values at ground level from Meteosat Second Generation (MSG) satellite images (Rigollier, Lefèvre, & Wald, 2004). Calculations for the irradiation values were based on data of the Horizontal Plane (global radiation), including day length and different irradiance measurement intervals (5 min, hourly, weekly and monthly) averaged from 1985-2005. The conversion from total irradiance (W/m²) to PAR (µmol/m²/s) was calculated manually according to McCree, 1981.

[5]**SoDa** (**so**lar radiation **da**ta), Integration and exploitation of networked Solar radiation Databases for environment monitoring
www.soda-is.com

4. Results and Discussion

The results of biomass production for wildtype and S5 are presented in Figure 9. Both cultivations were done under similar conditions, with both showing a growth phase up to day 2, this time interval was used to estimate the growth rate (μ, d^{-1}) and the biomass productivity (P_{cx}, g/L/d, Table 4). After the second light period all nitrogen was consumed by the cells, hence marking the start of the starvation phase (dashed line), in which starch and TAGs are produced.

4.1. Total biomass

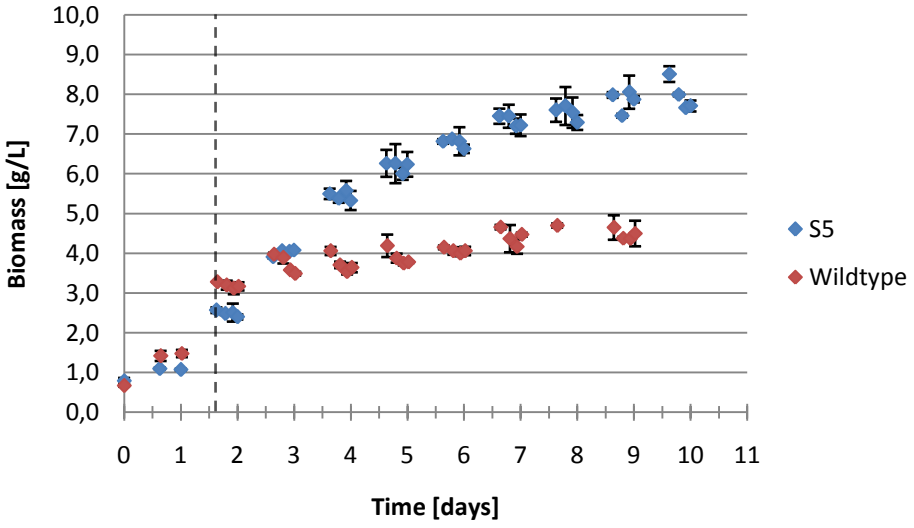

Figure 9: Concentration of total biomass in g/L (from DW measurements, see 3.4) for S5 and Wt. Nitrogen depletion is indicated with the dashed line after 1.6 days. Error bars indicate the sample deviations between the biological duplicates.

The biomass produced by S5 at the end of the cultivation was almost doubled (Fig. 9). The wildtype showed a stable biomass concentration after day 4, while S5 did not reach a stationary phase before the last two days in culture. Nitrogen depletion was reached in both cases after the second light period (1.63 d). As the initial nitrogen concentration was the same in both cases (125 ±1 g/L), the increase in biomass after nitrogen-depletion, is assumed to result solely from N-free biomass (non-functional biomass, in this case mainly TAGs and starch).

Nitrogen was only taken up during light periods, hence proteins, DNA, RNA in functional biomass were synthesized during daytime, since they require N in their composition. As the synthesis of proteins and chlorophyll are limited under N-starvation, the fraction (%) of functional biomass (X) in total biomass was declining over time as expected according

to previously published research (Pruvost, Van Vooren, Le Gouic, Couzinet-Mossion, & Legrand, 2011).

Loss of biomass during the nights was observed in both Wt and S5. *C. littorale* Wt reached a maximal night biomass loss (NBL) of 12 % (at onset of stationary phase) and an average loss of 7 % NBL (considering N-deplete cultivation period). *C. littorale* S5 showed lower values of night biomass losses, reaching a maximum NBL of 7 % (day 2) and an average NBL of 3 %. The model shows that the wildtype is cultivated with higher maintenance requirements (Wt: 1.8 E-06, S5: 8.8 E-07, see Appendix Tab. 6). According to the mechanistic model, primarily accumulated starch is degraded during nights to cover maintenance requirements. A calculation on the starch degradation rate during night of Wt and S5 showed that the NBL can be entirely described to starch degradation (g degraded STA/g DW before night, Wt: 7%, S5: 3 %), hence no other components are partaking to cover maintenance requirements.

All in all the greater amount of produced biomass in S5 can be ascribed to the increased TAG concentration, which proportionally increased the total biomass as well. In addition to that a lower maintenance requirement from S5 in comparison to Wt resulted in a lower NBL.

4.2. Biomass constituents

Concentrations of the biomass constituents TAG and starch from indoor experiments with Wt and S5 are shown in Figure 10. Nitrogen depletion was reached after 1.6 days, after that starch and TAGs are accumulated during nitrogen starvation.

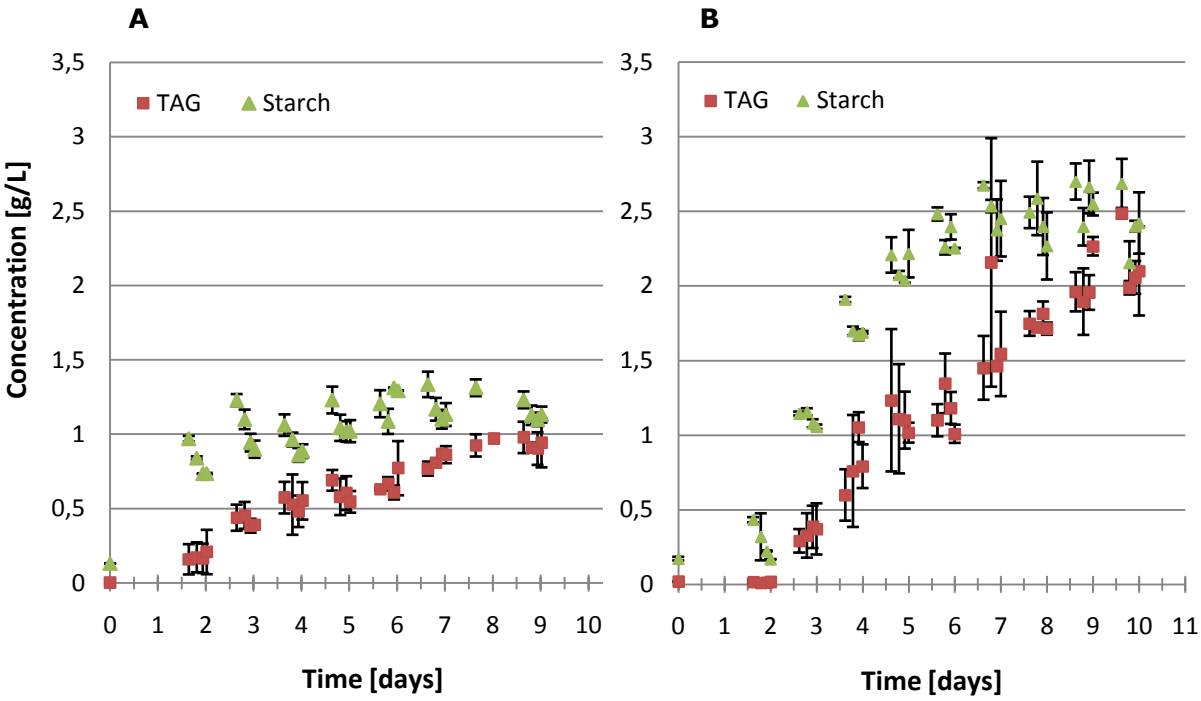

Figure 10: Concentrations of TAG and starch in Wt (A) and S5 (B) in g/L, including standard deviations between biological duplicates.

The comparison of biomass composition between Wt and S5 indicates an alteration in the carbon metabolism, since more TAGs are produced by S5. The average contents of starch and carbohydrates (% DW) stayed the same (see Table 4), but the relation between TAG and starch synthesis was improved towards TAG production. The TAG concentration was increased 2.5-fold in S5 (highest amounts see Table 4), the final relation of TAG:starch was 0.80:1 for Wt and 0.93:1 for S5. Due to the doubling increase of biomass in S5, the total concentration (g/L) of STA and CHO almost doubled in both cases respectively.

TAG concentrations in S5 were additionally improved by lower maintenance requirements (derived by model, Table 6). Under similar light conditions, less starch needed to be degraded during night respiration, leaving a higher fraction of starch available for conversion into TAGs during daytime, expressed by a higher starch to TAG conversion rate (rSTATAGmax Wt: 1.8 E-06; rSTATAGmax S5: 2.2 E-06, Tab. 6).

The present results also confirms the previous findings that S5 has an improved TAG content of S5 under continuous light. S5 was created via cell sorting, without any genetic

engineering, which clearly has its advantages, especially when the algae is aimed at the commodity markets, since no extra clearings for genetically modified organisms have to be passed. This can be an essential selling point within the food and feed market, without any extra costs caused by GMO regulations.

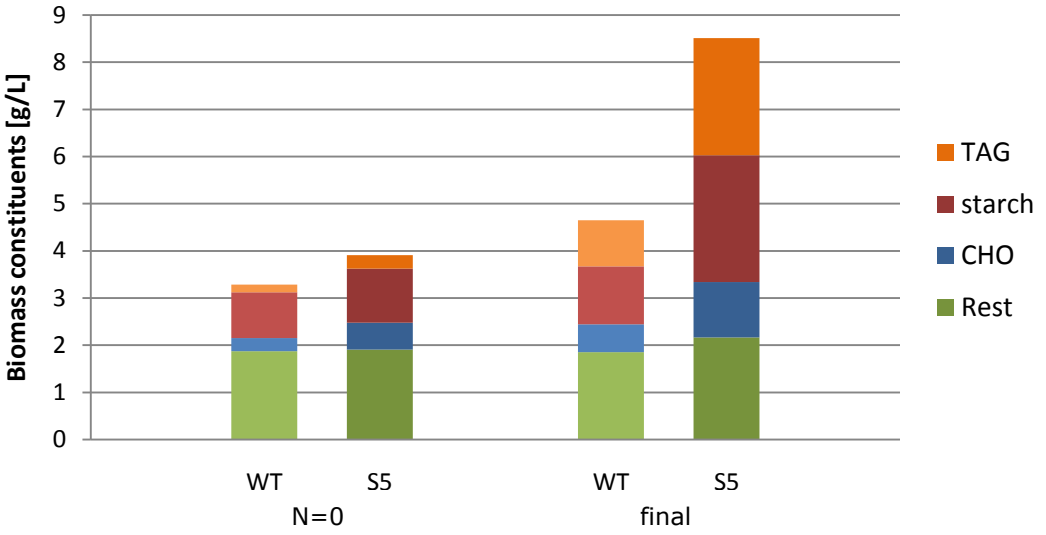

Figure 11: Concentrations (g/L) of biomass constituents TAG, starch, CHO (other carbohydrates then starch) and the residual biomass at the onset of nitrogen depletion (N=0) and at the end of the starvation phase (final) for Wt and S5.

Li and co-authors (Li, Han, Sommerfeld, & Hu, 2011) suggested that an increasing TAG productivity is linked to a higher production of starch and carbohydrates as well. As the cells diameter is increasing with a higher amount of accumulated lipid bodies, carbohydrates are used for enlarging the cell walls. The content of carbohydrates appeared unstable in both Wt and S5. After nitrogen depletion the CHO content seemed to stabilize, whereas later measurements are not conclusive whatsoever. It is assumed that the general carbohydrate concentration (without starch) is stable after N-starvation and the determination method is not reliable enough. Breuer et al. (2015) assumed that no functional biomass is produced after nitrogen depletion and the carbohydrate levels kept constant throughout the N-starvation. As experiments in current and previous works could not confirm this trend due to methodical problems[6], the observed average of 14 % (g/g DW) CHO in both cultivations were assumed to be stable during cultivation. Another aspect to the seemingly rising CHO contents are the findings of (Chihara et al., 1994), stating that the cell walls of *C. littorale* are thickening with age, which could lead to a general CHO increase over time.

[6] Protocol for total carbohydrate measurements (adapted from Dubois, described in 3.4) was not optimized and is under revision, as high standard deviations throughout experiments of the whole workgroup appeared.

4.3. Productivities

Table 4 provides an overview of productivities and yields of biomass and its constituents for the indoor experiments of Wt and S5 as well as the outdoor experiment with Wt.

Table 4: Overview of growth parameters, biomass and TAG productivities, yields of biomass and TAG on photons for indoor experiments with Wt and S5 as well as the Wt outdoor experiment.

	Unit	Timepoint	Wt	S5	Outdoor (Wt)
DLI	mol/d		4.40	4.40	138.5
final DW	g/L		4.65	8.51	4.28
μ	d^{-1}	t=0 - N=0	0.69 ± 0.04	0.72 ±0.07	0.45
P_{cx}	g/L/d	t=0 - N=0	1.04 ± 0.18	1.09 ±0.09	0.64
	g/d	t=0 - N=0	1.87 ± 0.32	1.97 ±0.16	57.82
$Yield_{cx,ph}$	g cx/ mol ph	t=0 - N=0	0.43 ± 0.07	0.45 ±0.04	0.42
Average NBL	g/g DW	N=0 - t=9	6.9 % ± 1 %	3.1 % ± 0.2 %	9.3 %
highest TAG concentration and content	g/L	t=9.65 d	0.93 ±0.02	2.49 ±0.05	0.64
	%	t=9.65 d	21.0%	29.2 % ± 0.1 %	15 %
$P_{TAG,max}$	g/L/d	t after N=0	0.28 ±0.005	0.40 ±0.09	0.11
	h	t after N=0	0-24	0-72	0-24
$P_{TAG,ave}$	g/L/d	N=0 - t=9	0.104 ±0.014	0.309 ±0.004	0.068
$Yield_{TAG, max}$	g TAG/ mol ph		0.114 ± 0.00	0.166 ±0.00	0.124
$Yield_{TAG, avg}$	g TAG/ mol ph		0.040 ±0.001	0.126	0.044
average STA	g/L	N=0 - t=9	1.03 ±0.16	1.96 ±0.09	0.61
	%	N=0 - t=9	27 % ± 3 %	30 % ± 0.9 %	18 %
average CHO	g/L	N=0 - t=9	0.56	0.87 ± 0.007	1.01
	%	N=0 - t=9	14.0 %	14.0 % ± 0.75 %	28.8 %

As described earlier in 4.2 biomass productivity is the same for S5 and Wt as the additional 4 g of final biomass completely accounts from increased concentrations of accumulated TAG and starch after nitrogen depletion. Average starch concentration increased 2-fold and final TAG concentration increased 2.5-fold in S5.

A comparison between the indoor and outdoor cultivation of *C. littorale* Wt shows a lower final concentration of total biomass after the outdoor run. This was expected due to a lower light intensity outside, however, the similar yields (biomass and TAGs) confirmed that the biological functions responded similar between indoors and outdoors cultivation.

Another factor that causes a difference between indoor and outdoor experiments is the design of the reactor, while indoor a flat panel reactor (0.02 m light path) was used, outdoors experiments were carried out in a tubular photobioreactor (0.05 m light path). A dense outdoor culture in a tubular system induces layers with different light supplies, hence a self-shading effect decreases biomass productivities and the photosynthetic rate (further discussion in 4.6).

A comparison of the TAG yields (maximum and average) between Wt and S5 shows a higher efficiency in making TAGs of S5. This was shown before, but a closer look reveals a substantial difference between average TAG productivities (and yields) and time-averaged maximum productivities (and yields) between the strains. TAG_{max} describes the average productivity/yield from the start of TAG production until the maximum productivity is reached (Wt and outdoor after 24 h, S5 after 72 h). In this time-frame the $P_{TAG,max}$ for S5 was 1.5-fold higher when compared to Wt. When calculating the average TAG productivity ($P_{TAG,avg}$, from start of TAG production until end of cultivation) however, a 2.6-fold increase in S5 compared to Wt was observed. This showed again that TAG accumulation in S5 were sustained over time without a major decrease in productivity. On the other hand this fact means also that the ideal cultivation period of S5 (e.g. in a semi-continuous cultivation) is 2 days longer than the wildtype.

4.4. Absorption cross section

The efficiency of a cell to absorb light gives an indication about the cellular pigmentation, and eventually light saturation. Figure 12 shows the absorption cross section over time for both WT and S5.

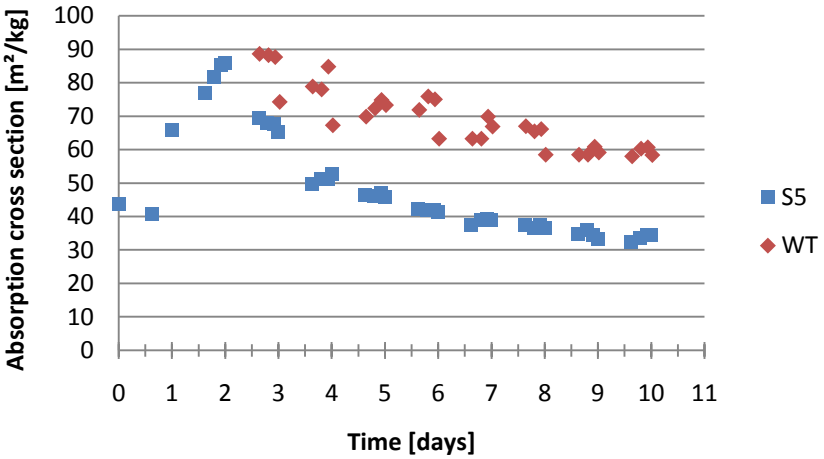

Figure 12: Absorption cross section (m²/kg) over time (days) for Wt and S5, no data is shown for the wildtype before the measurement at day 2.65 (not available).

The absorption coefficient reflects the light absorption of the cells. A reduced light absorption stands for a reduced content of cellular pigmentation (Pruvost et al., 2009; Solovchenko et al., 2013). The differences observed in the absorption gradient are not the result of a change in a metabolic mechanism, but can be moreover explained with taking biomass and nitrogen concentrations into consideration. The increased amount of total biomass in S5 (Fig. 9) mainly arose from the synthesis of N-free biomass, leaving a declining fraction of pigmentation behind, as *de novo* synthesis of chlorophyll was limited due to N-starvation (Pruvost et al., 2011). As the total dryweight is a divisor in the absorbance equation (Eq. 3), a lower cross section is inevitable. In other words, the lowered absorption cross section can be as well explained by the lowered cellular nitrogen content which is caused by a higher concentration of total biomass (Breuer et al., 2015; Geider, Macintyre, Graziano, & McKay, 1998) and are not essentially caused by a decreased photosynthetic efficiency. Quite the contrary was observed during the indoor experiments with Wt and S5, as S5 obtained much higher biomass and TAG yields on light.

4.5. Model simulations

The experimental data presented above were used to calculate the necessary input parameters for the model simulations (overview in Appendix, Table 6). The mechanistic model (Breuer et. al, 2015) has to be validated for growth and productivity estimations of *C. littorale* under simulated Dutch summer, as it was originally developed for *S. obliquus* under continuous light.

Model simulations and experimental data of total biomass, TAG and starch concentrations for the *C. littorale* wildtype can be seen in Figure 13.

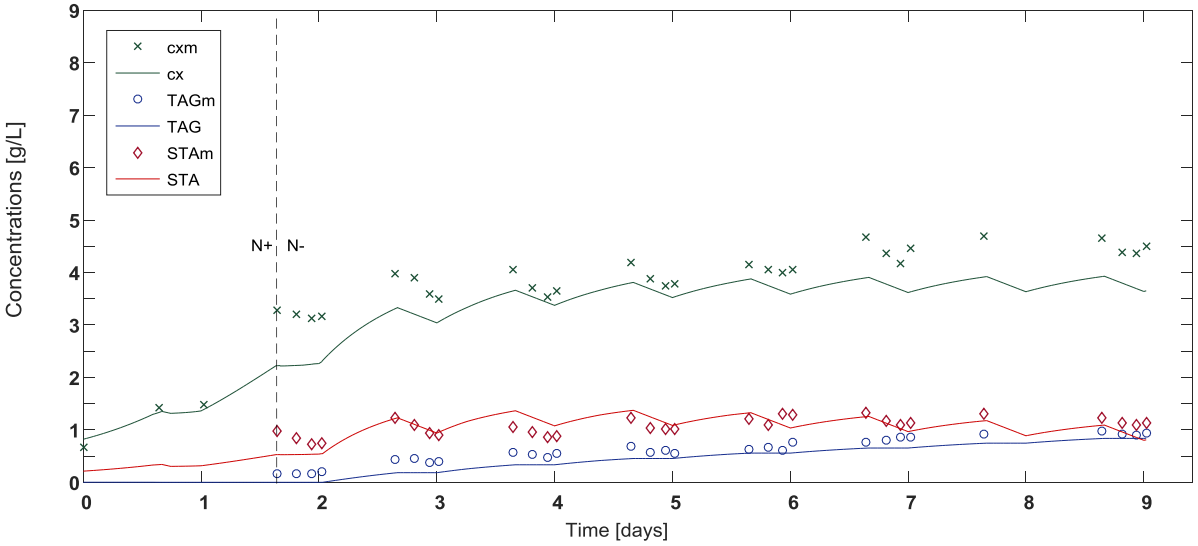

Figure 13: Model simulations for *C. littorale* Wt. Nitrogen depletion is indicadted through the dashed line. Experimentally derived concentrations (g/L) of total biomass (cx), TAG and starch (STA) are shown as single points, equivalent estimations by the model with a line in the corresponding colour.

Nitrogen depletion was reached after 1.63 days and the modelled biomass concentration at the onset of nitrogen depletion is underestimated. The total biomass was lightly underestimated throughout the whole cultivation period, especially regarding the last cultivation days.

The simulated TAG concentration was slightly underestimated but generally followed the experimental data. A steady increase of TAGs after nitrogen depletion without any degradations was both measured and simulated. The model showed a considerable starch degradation during nights which reflected the experimental data. After a starch concentration above 1 g/L is reached on day 4 (light period), the accumulated starch levels remained stable (with exception of the night respiration) with an average of 1.03 g/L after nitrogen depletion (see Table 4).

Both experimental and simulated data showed that starch is degraded during night (to cover maintenance requirements) and therefore caused a biomass (cx) loss. A comparison between Fig. 13 and Fig.14 showed a higher degradation of starch in the wildtype than S5, due to its higher maintenance demands (and consequently higher NBL; Tab. 4). The maintenance requirements could be theoretically covered by TAG degradation as well, but the resulting energy yields in terms of adenosine triphosphate (ATP) (60.7%) from TAGs is lower than the one of starch (65.3-66.7%) (Johnson & Alric, 2013), which explains why starch is used primarily to cover the maintenance requirements of *C. littorale*. All other biomass components (TAG, CHO, functional biomass) are consequentially assumed to stay stable during nights. Such assumption is confirmed by the stable concentrations of biomass components during the dark periods.

Fig. 14 shows measured and simulated data of total biomass (cx), triacylgylcerol (TAG) and starch (STA) concentration for S5. Experimental nitrogen depletion was reached after 1.6 days in accord with its simulation (see dashed line in Fig 14).

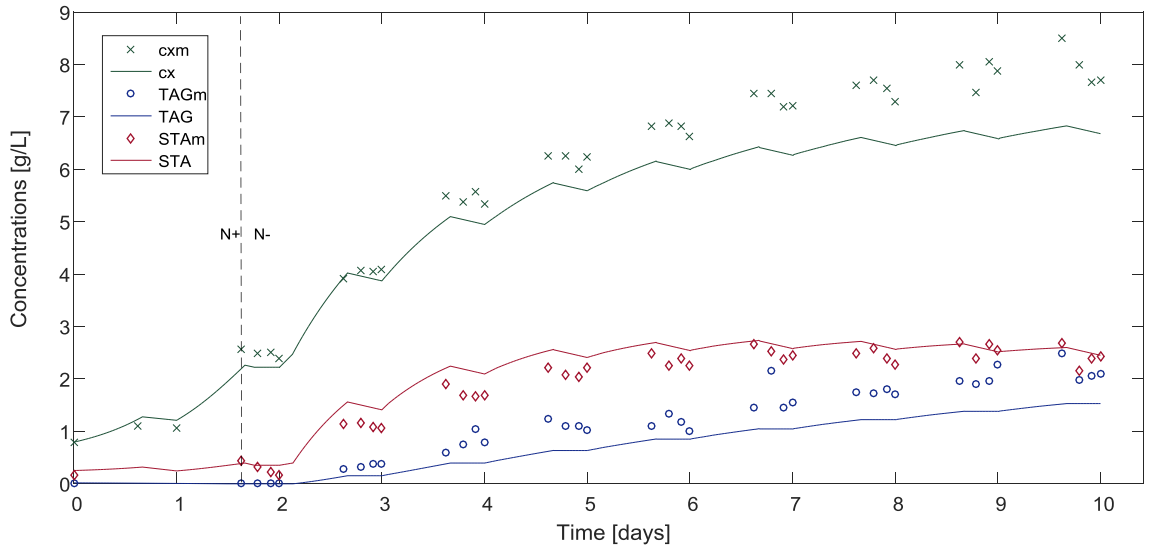

Figure 14: Model simulations for *C. littorale* S5. Nitrogen depletion is indicadted through the dashed line. Experimentally derived concentrations (g/L) of total biomass (cx), TAG and starch (STA) are shown as single points, equivalent estimations by the model with a line in the corresponding colour.

Total biomass and TAG production are underestimated by the model. The biomass growth is simulated according to the measured values until day 4. Cx during the last 5 days of cultivation is increasingly underestimated, whereat several factors could play a role in this process. No validations for the theoretical yields on an improved strain like S5 are yet made. The maximum theoretical yields were assumed to be still holding, but further metabolic research would have to be made for confirming those assumptions. The same factor might influence the underestimation of TAG production, with a final estimated content of 1.53 g/L and a measured value of 2.1 g/L .

A sensitivity analysis done by Wieneke (2015) revealed the two model parameters pA and pB as the most critical parameters for the partitioning between starch and TAG accumulation. Experienced problems within the pA/pB determination might leave an underestimated fraction of energy for TAG synthesis, in addition to the possibly underestimated theoretical yields.

The simulation followed closely the experimental starch measurements and showed a discreet degradation during nights after cultivation day 3. The starch levels are kept constant after 5 days of cultivation. Additionally, the confidence intervals (CI) between simulated and experimentally measured parameters were calculated for both Wt and S5 (Appendix, Tab. 6).CHO and STA have larger confidence intervals than other parameters, but yet STA presents most of the points within the interval. Most importantly, the concentrations of biomass and TAGs presented both acceptable confidence intervals, pointing to more reliable estimations that could be further used to extrapolate the simulated results.

4.6. Outdoor experiment

Results of the outdoor run with the wildtype of *Chlorococcum littorale* are shown in Fig. 15. Measured data for total biomass (cx), TAG, and starch concentrations are displayed with the simulated data respectively.

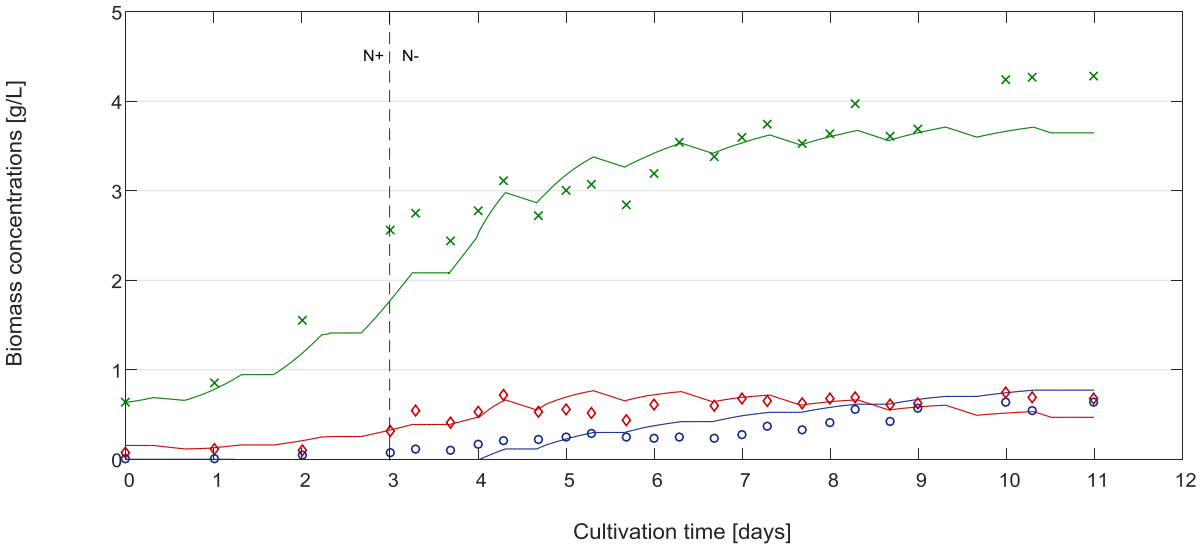

Figure 15: Model simulations for outdoor experiment with *C. littorale* Wt. Nitrogen depletion is indicadted through the dashed line. Experimentally derived concentrations (g/L) of total biomass (cx), TAG and starch (STA) are shown as single points, equivalent estimations by the model with a line in the corresponding colour.

Simulated total biomass concentration followed closely the experimental measurements, with an underestimated biomass concentration between day 2 and 4 (around onset of N-

depletion), that was already observed at the Wt indoor experiments model (see Fig. 13). The highest biomass concentrations reached just over 4 g/L and are thereby laying just below the value of the indoor runs with *C. littorale* wildtype. A comparison with the indoor runs showed a lower growth rate (μ, Table 4) and thereby a decreased biomass productivity. The yields (g cx/ mol photon, Tab. 4) however remained nearly the same, due to the lower light intensities outdoors (34.62 mol/m²/day)[7] when compared with indoor experiments (55 mol/m²/day). This situation combined with the differences in reactor design and volume caused a longer lag phase and hence the lowered growth rate. The same goes for the comparison of TAG concentration and yield between indoor and outdoor cultivations of Wt. The final TAG concentration of 0.64 g/L (15 % g/g DW) is significantly lower (WT indoor: 0.93 g/L, 21 %), while the overall TAG yield stayed the same (both 0.04 g TAG/ mol photon).

Benvenuti et. al. (2015) aimed for TAG production with *Nannochloropsis* sp. in a nitrogen runout batch cultivation using a similar horizontal tubular reactor (as for outdoor experiments within this project). Maximum TAG productivities (depending on initial biomass concentration) of 0.08-0.19 g TAG/mol photons were reached. The maximum TAG production ($P_{TAG,max}$, Tab. 4) reached during outdoor experiments with *C. littorale* was 0.11 g/mol and lays thereby in the same magnitude.

The outdoor experiment showed almost half the content of starch (18 %) and almost doubled average carbohydrate (excluding starch) content (29 %) compared to the indoor experiments (Tab. 4). The decreased starch content might be an indication of higher maintenance requirements, as it is firstly used to cover the cells energy demands overnight. The maintenance parameter (ms) was fitted in a MATLAB simulation depending (amongst all other experimentally derived input parameters) on a light scenario for a flat panel PBR, hence ms for the outdoors experiment underlay some model limitations. As the mechanistic model was designed for a flat panel reactor with a short light path, no self-shading effect of the cells was included in the estimation of ms. In a tubular outdoor system with a light path of 0.05 m, different irradiated layers occur, which lead to varying photosynthetic efficiencies. In addition to that is the light angle (under which sunlight impinges the reactor surface) an important parameter of the outdoor experiments, that is not incorporated in the model. The maintenance requirements (ms) estimated by the model could significantly differ from its actual value as some of the ms defining parameters are not included in the simulations.

As the total biomass simulation closely followed the experimental data, the present ms parameter is assumed to be holding for the simulations, despite the above mentioned

[7] Solar irradiation at ground level was measured at the pilot site

points. An increased fraction of starch was synthesized due to the lower light intensities outdoors, leaving less energy from absorbed photons for TAG and starch synthesis.

The simulation of TAG and starch concentrations are generally following the measured data. While the estimation of TAGs did not fit during the middle of cultivation, where no TAG increase was observed, values converged again towards the final TAG concentrations (day 10 and 11, simulated final TAG concentration: 0.73 g/L; measured final TAG concentration: 0.64 g/L). Starch simulation showed a declining trend towards the end of the cultivation which did not reflect the measured concentrations (Fig. 15).

Total biomass in the outdoor systems showed the highest night biomass loss, with an average NBL of 9.3 % dryweight (after N-depletion, Tab. 4). Starch was degraded overnight to cover the maintenance requirements which are in the same magnitude as for indoor experiments, but since the outdoor experiment was under lower light intensities than the indoor experiments it resulted in less energy left to synthesize carbon storage compounds (STA and TAG).

An important factor that the model does not incorporate is the influence of temperature. For general future scenarios a temperature controlled system is assumed to keep the temperature at optimum intervals. The pilot run for *C. littorale* reached maximum temperatures of about 32 °C on a daily basis throughout the whole cultivation time (with an average 7±2 h above 30 °C each day). Chihara et al. (1994) reported a lethal temperature maximum of 30 °C, which can be contradicted by the findings of this experiment. A negative impact on growth rate and yields are in any case not to be disregarded, but the unstable light supply during outdoor experiments are more likely to affect lipid metabolism. The metabolic priority is to fulfill the maintenance requirements, followed by production of starch that is used to fulfill the maintenance in the dark periods, which is showed by the starch reduction accounting for NBL.

In contrary to the indoor experiments the light supply did not remain stable throughout the cultivation, the average amount of light between day 5 and 7 was 29.6 mol/m²/day, which is laying 15 mol/m²/day under the average of the total cultivation period. This circumstance might be accountable for the pause of TAG production from day 5 to 7, which could have reduced the time-averaged TAG yield when compared with indoor experiments (0.044 gTAG/mol ph., compare Tab. 4). The model for this outdoor simulation was extended by incorporating the variations of the recorded daily light intensities, yet the estimations did not react to those changes and simulated a steady TAG accumulation.

Variations in the daily irradiation is a primary factor on photosynthesis, but a dense outdoor algae culture is sectioned into layers of different light supply due to reactor design, culture depth, cell concentration and mixing rate. This self-shading effect of the cells is decreasing the biomass productivity as low-light adapted cells (from the darker zones in culture) show a lowered photosynthesis rate (Tredici, 2010). No studies on photoacclimation and the regulation of photosynthesis has been done so far on *Chlorococcum littorale*. Cellular pigmentation changes over time to adapt to a changing light regime in most species, but (Havelková-Doušová, Prášil, & Behrenfeld, 2004) observed an acclimation of outdoor cultures exclusively to low light conditions. Richmond (2004) observed that the exposure of the cells to high irradiances (especially in the middle of the day) in the superficial layers is too short for the culture to adapt and photoinhibition occurs at surface. While on the other hand photosaturation might be reduced through varying irradiances at surface, leading to higher efficiencies under lower light levels during morning and late evening hours (Richmond, 2004). An adaptation of the cells to high irradiance does not seem possible if cultivated in a dense culture, even cells grown under continuous high light intensities would readapt within a few hours if transferred to outdoor conditions (Vonshak & Torzillo, 2004). Yet a partial adaptation to different climates can generally not be excluded as no experimental studies in different climates exist for *Chlorococcum littorale* and more research has to be performed. Since the model describes only the average daily productivity, actual measurements of the physiological state of the cells throughout the day were not carried out (and total irradiance is incorporated in the model as a block and not as a sinus).

For a final evaluation of the ability of the model to estimate outdoor cultivation with parameters derived from indoor experiments, the simulations based on indoor and outdoor cultivation were compared. Hence, figure 16 shows the same simulation and experimental data from outdoors as shown in figure 15, with the addition of another simulation line. This new simulation line was estimated from parameters derived from the indoor experiment (Wt), but using the light values calculated for the location of Wageningen.

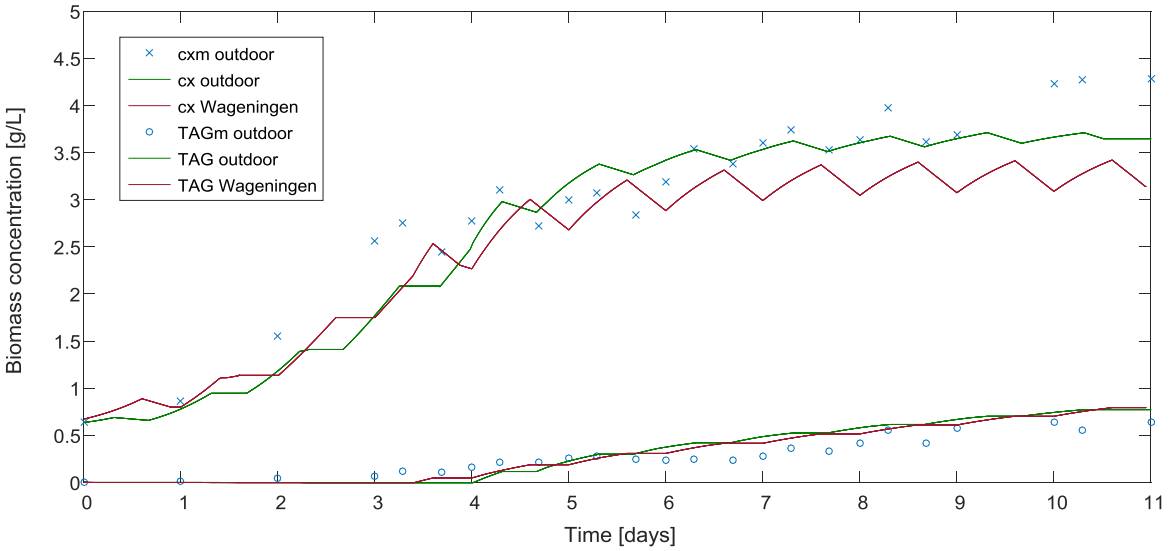

Figure 16: Experimental measurements of outdoor cultivation using Wt for total biomass (cx) and TAG concentration (g/L) are displayed as single points. Model simulations based on outdoor experimental parameters are shown in green; model simulations based on indoor experiments with adapted light values for Wageningen (location simulation) are shown in red.

The TAG simulations were nearly similar to each other and followed the experimental data. While the total biomass of the location simulation showed the same trend during growth phase, cx was underestimated in stationary phase.

The confidence intervals (CIs) were calculated to evaluate the accuracy of the estimations compared with the experimental data (Appendix, Tab. 6). The CIs of the outdoor experiment were higher than in comparison with the indoors experiments, but yet acceptable for Cx and TAG concentration, both the variables of interest in this work.

The differences in estimations of total biomass can be mainly ascribed to the different maintenance requirement (ms) used of the two simulations. Based on indoor experiments a much higher maintenance of the cells was observed (compare Tab. 6), leading to higher night biomass losses through respiration. This observation makes clear that maintenance requirements have to be experimentally derived for any further outdoor simulations under different climates, hence the following location simulations are estimating the potential for each location.

In summary, the mechanistic model by Breuer (2015) is valid for *C. littorale.* Estimations of indoor experiments with the wildtype followed closely the measured data. Biomass and TAG estimations for S5 were marginally underestimated and attention should be paid to the calculation of carbon partitioning parameters pA and pB. The simulation of the outdoor experiment followed closely the experimental data. As the model is however designed for cultivation in a flat panel PBR, outdoor simulations cannot be validated and just serve as potential estimations, or further adjustments in the model should be

implemented to correct the light regime of outdoor simulations. A good example of a potentially successful approach is the growth model by Slegers et al. (2013), which includes location specific irradiance and solar angles, advanced parameters of reactor design (e.g. materials, tube diameters, distance between tubes etc.) and species specific parameters to predict production yields in large scale tubular reactors. It gives a good example for the incorporation of advanced light scenarios outdoors, even though carbon partitioning is not included as no nitrogen starvation is considered.

The mechanistic model used for this work incorporates already important factors for successful outdoor estimations, while several additions need to be incorporated. The effect of light saturation is an important factor for outdoor simulations and already included through a photosynthesis-irradiance response curve (depending on absorption cross section and maximum photosynthetic rate q_{ph}^{max}) (Breuer et al., 2015). Due to the different reactor set-up outdoors, additional model parameters for the light supply should be implemented. The model by Breuer et. al. (2015) is one of the few model approaches not focusing on either photosynthesis or carbon partitioning, but combining both as a necessity to include a response to nitrogen starvation. One of the most obvious parameters not included in the model is certainly the effect of temperature. Even though it is assumed that possible future production facilities have controlled temperature, an automated cooling system might not always be feasible. Changing temperature has a significant effect on biomass growth, TAG accumulation and night biomass loss, hence an incorporation in the model could have a major impact on outdoor simulations (Breuer, Lamers, Martens, Draaisma, & Wijffels, 2013; Michels, Camacho-Rodríguez, Vermuë, & Wijffels, 2014; Ota, Takenaka, Sato, Lee Smith, & Inomata, 2015).

4.7. Model simulations at different locations

After the validation of the model for simulations on *C. littorale*, the potential for cultivation under different light regimes was tested. Considering that the outdoor simulations showed acceptable confidence intervals for both biomass (N+) and TAG (N-) concentrations, it is assumed that the mechanisms described from the indoors experiments would be valid under outdoors conditions. Hence, the initial biological parameters and growth conditions from the indoor experiments were used to estimate the productivities of both Wt and S5 under the light regime of different locations.

Model parameters derived from the indoor experiments in flat panel PBR for both Wt and S5 were combined with the light values (light intensity and day length) for Wageningen, Oslo, Rio de Janerio and Cádiz. Figure 17 shows the average daily amount of light for each location.

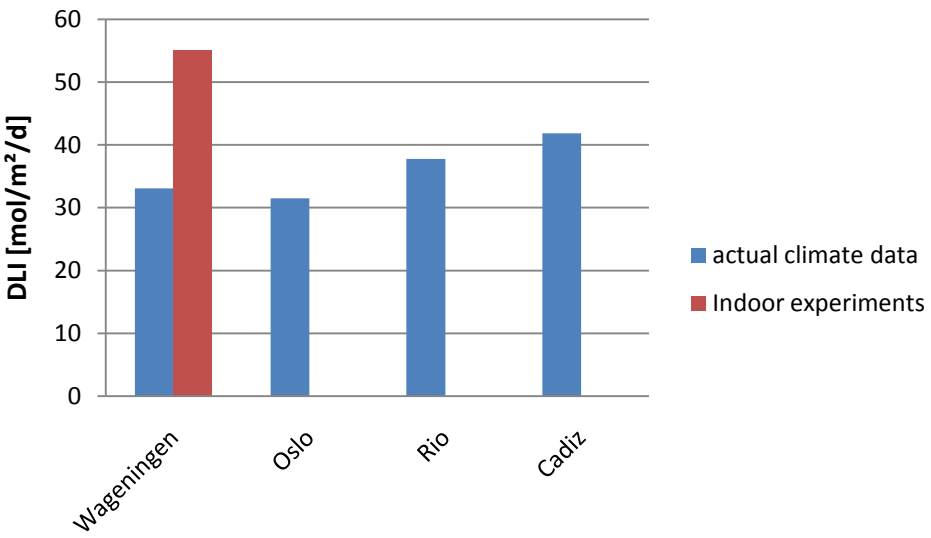

Figure 17: Daily light integral (mol/m²/day) for the locations Wageningen, Oslo, Rio and Cadiz as well as for the indoor experiments simulating a dutch summer day.DLI for Wageningen and Oslo are averages for the cultivation period from April to August, while an average DLI of the whole year are shown for Rio and Cádiz (compare M+M. 3.6). The red bar shows the DLI of the indoor experiments, resulting of a 16 h light period with an intensity of 1500 µmol/m²/s.

A nitrogen runout batch cultivation was assumed equivalent to the experiments, hence the maximum (final) concentration of functional biomass was expected to be alike in all scenarios. Accumulation of TAG and starch after nitrogen depletion are however dependent on photosynthesis rate of each location (carbon partitioning between starch and TAG is unchanged through the same set of model parameters). Hence, the yields of both biomass and TAG are solely dependent on light intensity and duration of the day. Yields on light and productivities are shown in Table 5 for both Wt and S5.

Table 5: Concentrations, productivites (P) and yields of total biomass (cx) and TAG for Wt and S5 in the locations of Oslo, Wageningen, Rio and Cádiz. Production periods from April-August are assumed for Oslo and Wageningen, whole-year production for Rio and Cádiz.

	Unit		Oslo		Wageningen		Rio		Cádiz	
			WT	S5	WT	S5	WT	S5	WT	S5
Daylength	h		16.5		15.2		12.0		12.0	
DLI	mol/m²/d		32		33		38		42	
	mol/d		2.5		2.6		3.0		3.3	
N-depletion	d		3.23	2.27	3.32	2.32	4.09	3.02	4.03	3.03
final DW	g/L		3.59	6.59	3.58	6.45	3.45	6.17	3.50	6.21
μ	d^{-1}		0.39	0.53	0.38	0.50	0.33	0.46	0.33	0.46
P_{cx}	g/L/d		0.47	0.71	0.38	0.64	0.41	0.67	0.42	0.67
$Yield_{cx,ph}$	g Cx/ mol ph		0.48	0.51	0.53	0.44	0.24	0.40	0.23	0.36
max TAG conc.	g/L		0.69	1.25	0.74	1.25	0.75	1.17	0.79	1.20
$P_{TAG,max}$	g/L/d		0.24	0.21	0.22	0.23	0.29	0.27	0.30	0.28
$P_{TAG,\ avg}$	g/L/d		0.11	0.17	0.12	0.17	0.14	0.18	0.14	0.18
$Yield_{TAG,avg}$	g TAG/mol ph		0.08	0.12	0.08	0.12	0.08	0.11	0.08	0.10
theoretical max TAG conc.	Wt: 21 % S5: 29 %	g/L	0.75	1.93	0.75	1.88	0.73	1.80	0.74	1.81
$P_{TAG,avg,theo.}$	g/L/d		0.12	0.23	0.12	0.21	0.13	0.27	0.13	0.28
$Yield_{TAG,theo.}$	g TAG/mol ph		0.09	0.16	0.08	0.15	0.08	0.14	0.07	0.13

Final biomass concentrations were estimated as expected without major differences among the difference locations. When it comes to final TAG concentrations, the lowest values are estimated in Oslo with just about 10 % less content as the highest value, which was in Cádiz. The maximum and average productivity of TAGs is accordingly highest in Rio and Cádiz and lowest values are observed in Oslo. This is caused through a later time point of nitrogen depletion in Rio and Cádiz, with a similar amount of TAGs being produced in less time. Interestingly enough, the maximum TAG concentrations of Wt and S5 are not obtained in the same locations. While the wildtype is showing its lowest TAG concentration in Oslo and the highest in Cádiz, it is following the increasing light irradiance. An opposite pattern was observed with the S5 TAG concentration, with maximum values of Rio and Cádiz being slightly lower than maximum concentration in Wageningen and Oslo. The final TAG concentration (g/L) of S5 lays 1.5 (Cadiz) -1.8 (Oslo) -fold above the estimations for Wt.

When it comes to the overall TAG yield on light, no differences between the locations occurred for the wildtype, while the S5 TAG yields are slightly higher in Oslo and Wageningen then in Rio and Cádiz and 22-36 % higher than the Wt yields. The model

contains a photosynthesis-irradiance curve (determined through model parameters $q_{ph,max}$, absorbance coefficient and light intensity), which describes absorption of photons and the subsequent photosynthetic rate and thereby includes a light saturation effect as well. Breuer et al. (2013) is already describing substantial yield losses in the model species *Scenedesmus obliquus* under high light intensities. Both the comparison of indoor (high light intensities) and outdoor (lower light intensities) experiments, as well as the location simulations showed that light saturation occurred at high irradiances. The maximum biomass concentration is limited proportionally to the initial nitrogen concentration, which is resulting in a lowered photosynthetic efficiency at high irradiances. Most marine algae saturate already at light intensities below 100 µmol/m²/s (Tredici, 2010), hence just a fraction of received irradiance is actually utilized for photosynthesis. This means that the threshold of light saturation determines the maximum possible photosynthetic efficiency of a culture (Goldman, 1979). Kurano & Miyachi (2005) observed light saturation for *Chlorococcum littorale* from light intensities above 300 µmol/m²/s, determined by a light response curve (µ-I curve). Referring to the location simulations it explains why large increases in irradiance do not lead to proportional increasing TAG productivities. It has to be pointed out, that a production period from April-August was assumed for Wageningen and Oslo, making a direct comparison of yields with a year-round production in Rio and Cádiz unequable.

The higher TAG efficiency of S5 compared to Wt has to be highlighted, although both strains were affected by light saturation. As the simulations are based on model parameters derived from the indoor experiments, estimations of biomass and TAG concentrations are accordingly fitting or over-/underestimated as shown in Figure 13 and Figure 14. The simulation of TAG concentration for S5 (from indoors experiment) were clearly underestimated, which is leading to the assumption that the simulated TAG concentration (and hence TAG productivities and yields) for different locations are underestimated as well. To overcome this limitation, experimentally determined final TAG contents (Wt: 21 % g TAG/g DW; S5: 29 % g TAG/g DW) were multiplied by the model estimated final biomass concentrations, resulting in a set of theoretical TAG concentrations as shown in Table 4. The consequential theoretical productivities and yields for Wt remained similar to the values estimated by the model as expected (as TAG estimations for Wt showed a good fit in Fig. 13). The theoretical final TAG concentration for S5 however increased by 50-55%, which would be a 2.5-fold increase compared to Wt. As a 2.5-fold increased final TAG concentration in S5 was already observed in measurements from indoor experiments, the estimation of TAGs in S5 based on the experimentally determined TAG concentration combined with the by the model simulated biomass concentration is recommendable.

5. Conclusion

The results of the indoor experiments confirmed an increased TAG content of the sorted *Chlorococcum littorale* S5. A 2.5-fold increase of TAG concentration is clearly an improvement towards feasible microalgae production within the bulk commodity market. The mechanistic model is holding for the prediction of total biomass concentrations of *C. littorale* (for both Wt and S5) but could not be fully validated for S5 TAG concentrations. The altered carbon partitioning can be partly explained by lower maintenance requirements and further research have to validate or adapt the model parameters of theoretical maximum yields (for biomass constituents and conversion rates) for S5. The estimations of TAG and biomass concentrations are, however, within acceptable confidence intervals, assuring the use of modelled data.

The estimations of four different light simulations did not show major differences in TAG accumulation. TAG yields on light are decreasing at high light intensities, as light saturation lowered the photosynthetic efficiency. This fact shows that a production of *C. littorale* in southern latitudes are not naturally leading to higher productivities but could moreover be less feasible as shading and cooling technologies have to be applied. All in all, it can be concluded that allocating microalgae production should not rely solely to the light availability, as this and previous research have shown that microalgae cannot convert all impinging light and still can suffer from light inhibition during hours of peak irradiance.

6. Recommendations

For further modelling approaches with *C. littorale* S5 the maximum theoretical yields should be revised. TAG concentrations are underestimated and there is no evidence that the assumed theoretical yields are still holding for a sorted population with a changed carbon metabolism. As the biomass concentration however is reliably simulated, TAG estimations could be made using the final TAG content (%) from experimental data (as shown for estimations for different locations). Since differences in the TAG content of S5 appeared between indoor and outdoor simulations, experimental determination is still necessary for each scenario.

Future research should as well investigate a more efficient cultivation mode. Biomass and TAG productivity are reaching its maximum right after nitrogen depletion. A semi-continuous nitrogen limited process could lead to a stable high TAG productivity in larger production scales. A constant algae concentration should be kept through daily harvesting and a dilution with N-depleted biomass, that has been grown in a nitrogen runout preculture (Bona, Capuzzo, Franchino, & Maffei, 2014; Terigar & Theegala, 2014). A diluted culture could achieve a greater photosynthetic efficiency since a greater amount of impinging photons can be absorbed (Goldman, 1979; Richmond, 2004).

Simulations of locations with different light scenarios showed a decreasing biomass and TAG productivity under higher light intensities. An economical evaluation of the year-round productivity would be necessary, as maximum yields and productivities might be similar for different locations, without taking a yearly average into account. As production periods vary depending on latitude, microalgae production might not be feasible without a whole-year production, despite similar maximum productivities and yields. On the other hand should the extra TAG productivities at locations with high irradiances justify additional costs for shading and cooling to avoid photo inhibition.

7. References

Baquerisse, D., Nouals, S., Isambert, A., dos Santos, P. F., & Durand, G. (1999). Modelling of a continuous pilot photobioreactor for microalgae production. *Progress in Industrial Microbiology*, *35*(C), 335–342. doi:10.1016/S0079-6352(99)80125-8

Beckmann, J., Lehr, F., Finazzi, G., Hankamer, B., Posten, C., Wobbe, L., & Kruse, O. (2009). Improvement of light to biomass conversion by de-regulation of light-harvesting protein translation in Chlamydomonas reinhardtii. *Journal of Biotechnology*, *142*(1), 70–77. doi:http://dx.doi.org/10.1016/j.jbiotec.2009.02.015

Benvenuti, G., Bosma, R., Cuaresma, M., Janssen, M., Barbosa, M. J., & Wijffels, R. H. (2015). Selecting microalgae with high lipid productivity and photosynthetic activity under nitrogen starvation. *Journal of Applied Phycology*, *27*(4), 1425–1431. doi:10.1007/s10811-014-0470-8

Benvenuti, G., Bosma, R., Klok, A. J., Ji, F., Lamers, P. P., Barbosa, M. J., & Wijffels, R. H. (2015). Microalgal triacylglycerides production in outdoor batch-operated tubular PBRs. *Biotechnology for Biofuels*, *8*(1), 100. doi:10.1186/s13068-015-0283-2

Benvenuti, G., Lamers, P. P., Breuer, G., Bosma, R., Cerar, A., Wijffels, R. H., & Barbosa, M. J. (2016). Microalgal TAG production strategies : why batch beats repeated batch. *Biotechnology for Biofuels*, 1–17. doi:10.1186/s13068-016-0475-4

Berges, J. a., Charlebois, D. O., Mauzerall, D. C., & Falkowski, P. G. (1996). Differential Effects of Nitrogen Limitation on Photosynthetic Efficiency of Photosystems I and II in Microalgae. *Plant Physiology*, *110*, 689–696. doi:10.1104/pp.110.2.689

Bernard, O. (2011). Hurdles and challenges for modelling and control of microalgae for CO2 mitigation and biofuel production. *Journal of Process Control*, *21*(10), 1378–1389. doi:10.1016/j.jprocont.2011.07.012

Bona, F., Capuzzo, A., Franchino, M., & Maffei, M. E. (2014). Semicontinuous nitrogen limitation as convenient operation strategy to maximize fatty acid production in Neochloris oleoabundans. *Algal Research*, *5*(1), 1–6. doi:10.1016/j.algal.2014.03.007

Bowles, D. (2007). *Micro-and macro-algae: utility for industrial applications*. *Outputs from the EPOBIO project*. Newbury (UK): CPL Press.

Breuer, G., Evers, W. A. C., de Vree, J. H., Kleinegris, D. M. M., Martens, D. E., Wijffels, R. H., & Lamers, P. P. (2013). Analysis of Fatty Acid Content and Composition in Microalgae. *Journal of Visualized Experiments*, *80*(September), e50628. doi:10.3791/50628

Breuer, G., Lamers, P. P., Janssen, M., Wijffels, R. H., & Martens, D. E. (2015). Opportunities to improve the areal oil productivity of microalgae. *Bioresource Technology*, *186*, 294–302. doi:10.1016/j.biortech.2015.03.085

Breuer, G., Lamers, P. P., Martens, D. E., Draaisma, R. B., & Wijffels, R. H. (2012). The impact of nitrogen starvation on the dynamics of triacylglycerol accumulation in nine microalgae strains. *Bioresource Technology*, *124*, 217–226. doi:10.1016/j.biortech.2012.08.003

Breuer, G., Lamers, P. P., Martens, D. E., Draaisma, R. B., & Wijffels, R. H. (2013). Effect of light intensity, pH, and temperature on triacylglycerol (TAG) accumulation induced by nitrogen starvation in Scenedesmus obliquus. *Bioresource Technology*, *143*, 1–9. doi:10.1016/j.biortech.2013.05.105

Cabanelas, I. T. D., van der Zwart, M., Kleinegris, D. M. M., Barbosa, M. J., & Wijffels, R. H. (2015). Rapid method to screen and sort lipid accumulating microalgae. *Bioresource Technology*, *184*, 47–52. doi:10.1016/j.biortech.2014.10.057

Chihara, M., Nakayama, T., Inouye, I., & Kodama, M. (1994). Chlorococcum littorale, a New Marine Green Coccoid Alga (Chlorococcales, Chlorophyceae). *Archiv Für Protistenkunde*, *144*(3), 227–235. doi:10.1016/S0003-9365(11)80133-8

Chisti, Y. (2008). Biodiesel from microalgae beats bioethanol. *Trends in Biotechnology*, *26*(3), 126–131. doi:10.1016/j.tibtech.2007.12.002

Csögör, Z., Herrenbauer, M., Perner, I., Schmidt, K., & Posten, C. (1999). Design of a photo-bioreactor for modelling purposes. *Chemical Engineering and Processing: Process Intensification*, *38*(4), 517–523. doi:10.1016/S0255-2701(99)00048-3

de Jaeger, L., Verbeek, R. E., Draaisma, R. B., Martens, D. E., Springer, J., Eggink, G., & Wijffels, R. H. (2014). Superior triacylglycerol (TAG) accumulation in starchless mutants of Scenedesmus obliquus: (I) mutant generation and characterization. *Biotechnology for Biofuels*, *7*(1), 69. doi:10.1186/1754-6834-7-69

Draaisma, R. B., Wijffels, R. H., Slegers, P., Brentner, L. B., Roy, A., & Barbosa, M. J. (2013). Food commodities from microalgae. *Current Opinion in Biotechnology*, *24*(2), 169–177. doi:10.1016/j.copbio.2012.09.012

Durnford, D. G., & Falkowski, P. G. (1997). Chloroplast redox regulation of nuclear gene transcription during photoacclimation. *Photosynthesis Research*, *53*(2), 229–241. doi:10.1023/A:1005815725371

Fernandes, B., Dragone, G., Abreu, A. P., Geada, P., Teixeira, J., & Vicente, A. (2012). Starch determination in Chlorella vulgaris—a comparison between acid and enzymatic methods. *Journal of Applied Phycology*, *24*(5), 1203–1208. doi:10.1007/s10811-011-9761-5

Fukuda, H., Kondo, A., & Noda, H. (2001). Review: Biodiesel Fuel Production by Transesterification of Oils. *Journal of Bioscience and Bioengineefxng*, *92*(5), 405–416. doi:http://dx.doi.org/10.1016/S1389-1723(01)80288-7

Geider, R. J., La Roche, J., Greene, R. M., & Olaizola Miguel. (1993). Response of the photosynthetic apparatus of Phaeodactylum Tricornutum (Bacillariphyceae) to nitrate, phosphate, or iron starvation. *Journal of Phycology*, *29*(6), 755–766. doi:10.1111/j.0022-3646.1993.00755.x

Geider, R. J., Macintyre, H. L., Graziano, L. M., & McKay, R. M. L. (1998). Responses of the photosynthetic apparatus of Dunaliella tertiolecta (Chlorophyceae) to nitrogen and phosphorus limitation. *European Journal of Phycology*, *33*(4), 315–332. doi:10.1017/S096702629800184X

Goldman, J. C. (1979). Outdoor algal mass cultures-II. Photosynthetic yield limitations. *Water Research*, *13*(2), 119–136. doi:10.1016/0043-1354(79)90083-6

Grima, E. M., Pérez, J. A. S., Camacho, F. G., Medina, A. R., Giménez, A. G., & Alonso, D. L. (1995). The production of polyunsaturated fatty acids by microalgae: from strain selection to product purification. *Process Biochemistry*, *30*(8), 711–719. doi:http://dx.doi.org/10.1016/0032-9592(94)00047-6

Harris, W. S., Kris-Etherton, P. M., & Harris, K. A. (2008). Intakes of long-chain omega-3 fatty acid associated with reduced risk for death from coronary heart disease in healthy adults. *Current Atherosclerosis Reports*, *10*(6), 503–509. doi:10.1007/s11883-008-0078-z

Havelková-Doušová, H., Prášil, O., & Behrenfeld, M. J. (2004). Photoacclimation of Dunaliella tertiolecta (Chlorophyceae) Under Fluctuating Irradiance. *Photosynthetica*, *42*(2), 273–281. doi:10.1023/B:PHOT.0000040600.04502.32

Hu, Q. (2004). Environmental Effects on Cell Composition. In A. Richmond (Ed.), *Handbook of Microalgal Culture: Biotechnology and Applied Phycology* (pp. 83–93). Oxford: Blackwell Science Ltd.

Hu, Q., Kurano, N., Kawachi, M., Iwasaki, I., & Miyachi, S. (1998). Ultrahigh-cell-density culture of a marine green alga Chlorococcum littorale in a flat-plate photobioreactor. *Applied Microbiology and Biotechnology*, *49*(6), 655–662. doi:10.1007/s002530051228

Hu, Q., Sommerfeld, M., Jarvis, E., Ghirardi, M., Posewitz, M., Seibert, M., & Darzins, A. (2008). Microalgal triacylglycerols as feedstocks for biofuel production: perspectives and advances. *The Plant Journal*, *54*(4), 621–639. doi:10.1111/j.1365-313X.2008.03492.x

Jassby, A. D., & Platt, T. (1976). Mathematical formulation of the relationship between photosynthesis and light for phytoplankton. *Limnology and Oceanography*, *21*(4), 540–547. doi:10.4319/lo.1976.21.4.0540

Johnson, X., & Alric, J. (2013). Central carbon metabolism and electron transport in chlamydomonas reinhardtii: Metabolic constraints for carbon partitioning between oil and starch. *Eukaryotic Cell*, *12*(6), 776–793. doi:10.1128/EC.00318-12

Kirschbaum, M. U. F., Küppers, M., Schneider, H., Giersch, C., & Noe, S. (1998). Modelling photosynthesis in fluctuating light with inclusion of stomatal conductance, biochemical activation and pools of key photosynthetic intermediates. *Planta*, *204*(1), 16–26. doi:10.1007/s004250050225

Kliphuis, A. M. J., Klok, A. J., Martens, D. E., Lamers, P. P., Janssen, M., & Wijffels, R. H. (2012). Metabolic modeling of Chlamydomonas reinhardtii: Energy requirements for photoautotrophic growth and maintenance. *Journal of Applied Phycology*, *24*(2), 253–266. doi:10.1007/s10811-011-9674-3

Klok, A. J., Verbaanderd, J. A., Lamers, P. P., Martens, D. E., Rinzema, A., & Wijffels, R. H. (2013). A model for customising biomass composition in continuous microalgae production. *Bioresource Technology*, *146*, 89–100. doi:10.1016/j.biortech.2013.07.039

Kurano, N., & Miyachi, S. (2005). Selection of microalgal growth model for describing specific growth rate-light response using extended information criterion. *Journal of Bioscience and Bioengineering*, *100*(4), 403–408. doi:10.1263/jbb.100.403

Li, Y., Han, D., Hu, G., Dauvillee, D., Sommerfeld, M., Ball, S., & Hu, Q. (2010). Chlamydomonas starchless mutant defective in ADP-glucose pyrophosphorylase hyper-accumulates triacylglycerol. *Metabolic Engineering*, *12*(4), 387–391. doi:http://dx.doi.org/10.1016/j.ymben.2010.02.002

Li, Y., Han, D., Sommerfeld, M., & Hu, Q. (2011). Photosynthetic carbon partitioning and lipid production in the oleaginous microalga Pseudochlorococcum sp. (Chlorophyceae) under nitrogen-limited conditions. *Bioresource Technology*, *102*(1), 123–129. doi:10.1016/j.biortech.2010.06.036

Macintyre, H. L., Kana, T. M., Anning, T., & Geider, R. J. (2002). Review Photoacclimation of Photosynthesis Irradiance Response Curves and Photosynthetic Pigments in Microalgae and Cyanobacteria 1, *38*(July 2000), 17–38.

Mata, T. M., Martins, A. A., & Caetano, N. S. (2010). Microalgae for biodiesel production and other applications: A review. *Renewable and Sustainable Energy Reviews*, *14*(1), 217–232. doi:10.1016/j.rser.2009.07.020

McCree, K. J. (1981). Photosynthetically Active Radiation. In *Physiological Plant Ecology* (pp. 41–55). Heidelberg: Springer Berlin. doi:10.1007/978-3-642-68090-8_3

Michels, M. H. A., Camacho-Rodríguez, J., Vermuë, M. H., & Wijffels, R. H. (2014). Effect of cooling in the night on the productivity and biochemical composition of Tetraselmis suecica. *Algal Research*, *6*(PB), 145–151. doi:10.1016/j.algal.2014.11.002

Ohlrogge, J., & Browse, J. (1995). Lipid biosynthesis. *The Plant Cell*, *7*(7), 957–970. Retrieved from http://www.ncbi.nlm.nih.gov/pmc/articles/PMC160893/

Ota, M., Takenaka, M., Sato, Y., Lee Smith, R., & Inomata, H. (2015). Effects of light intensity and temperature on photoautotrophic growth of a green microalga, Chlorococcum littorale. *Biotechnology Reports*, *7*, 24–29. doi:10.1016/j.btre.2015.05.001

Parkhill, J., Maillet, G., & Cullen, J. J. (2001). Fluorescence-based maximal quantum yield for PSII as a diagnostic of nutirent stress. *Journal of Phycology*, *37*(4), 517–529. doi:10.1046/j.1529-8817.2001.037004517.x

Polle, W. J. E., Benemann, R. J., Tanaka, A., & Melis, A. (2000). Photosynthetic apparatus organization and function in the wild type and a chlorophyll b-less mutant of Chlamydomonas reinhardtii. Dependence on carbon source. *Planta*, *211*(3), 335–344. doi:10.1007/s004250000279

Pruvost, J., Van Vooren, G., Cogne, G., & Legrand, J. (2009). Investigation of biomass and lipids production with Neochloris oleoabundans in photobioreactor. *Bioresource Technology*, *100*(23), 5988–5995. doi:10.1016/j.biortech.2009.06.004

Pruvost, J., Van Vooren, G., Le Gouic, B., Couzinet-Mossion, A., & Legrand, J. (2011). Systematic investigation of biomass and lipid productivity by microalgae in photobioreactors for biodiesel application. *Bioresource Technology*, *102*(1), 150–158. doi:10.1016/j.biortech.2010.06.153

Ramazanov, A., & Ramazanov, Z. (2006). Isolation and characterization of a starchless mutant of Chlorella pyrenoidosa STL-PI with a high growth rate, and high protein and polyunsaturated fatty acid content. *Phycological Research*, *54*(4), 255–259. doi:10.1111/j.1440-1835.2006.00416.x

Reinhardt, G., Rettenmaier, N., & Köppen, S. (2008). *How sustainable are biofuels for transportation? In: Bioenergy: challenges and opportunities. International conference and exhibition on bioenergy*.

Richmond, A. (2004). Biological principles of mass cultivation. In A. Richmond (Ed.), *Handbook of microalgal culture: Biotechnology and applied phycology* (pp. 125–177). Oxford, UK: Blackwell Science Ltd.

Rigollier, C., Lefèvre, M., & Wald, L. (2004). The method Heliosat-2 for deriving shortwave solar radiation from satellite images. *Solar Energy*, *77*(2), 159–169. doi:10.1016/j.solener.2004.04.017

Rodolfi, L., Zittelli, G. C., Bassi, N., Padovani, G., Biondi, N., Bonini, G., & Tredici, M. R. (2009). Microalgae for oil: Strain selection, induction of lipid synthesis and outdoor mass cultivation in a low-cost photobioreactor. *Biotechnology and Bioengineering*, *102*(1), 100–112. doi:10.1002/bit.22033

Roessler, P. G. (1990). Environmental Commercial Control of Glycerolipid Metabolism Implications. *Journal of Phycology*, *399*(3), 393–399. doi:10.1111/j.0022-3646.1990.00393.x

Scarlat, N., Dallemand, J. F., & Pinilla, F. G. (2008). Impact on agricultural land resources of biofuels production and use in the european union. *Bioenergy: Challenges and Oppertunities. International Conference and Exhibition on Bioenergy*.

Scott, S. A., Davey, M. P., Dennis, J. S., Horst, I., Howe, C. J., Lea-Smith, D. J., & Smith, A. G. (2010). Biodiesel from algae: challenges and prospects. *Current Opinion in Biotechnology*, *21*(3), 277–286. doi:http://dx.doi.org/10.1016/j.copbio.2010.03.005

Slegers, P. M., Lösing, M. B., Wijffels, R. H., van Straten, G., & van Boxtel, A. J. B. (2013). Scenario evaluation of open pond microalgae production. *Algal Research*, *2*(4), 358–368. doi:10.1016/j.algal.2013.05.001

Slegers, P. M., van Beveren, P. J. M., Wijffels, R. H., van Straten, G., & van Boxtel, A. J. B. (2013). Scenario analysis of large scale algae production in tubular photobioreactors. *Applied Energy*, *105*, 395–406. doi:10.1016/j.apenergy.2012.12.068

Solovchenko, A., Solovchenko, O., Khozin-Goldberg, I., Didi-Cohen, S., Pal, D., Cohen, Z., & Boussiba, S. (2013). Probing the effects of high-light stress on pigment and lipid metabolism in nitrogen-starving microalgae by measuring chlorophyll fluorescence transients (Chlorophyta, Trebouxiophyceae). *Algal Research*, *2*(3), 175–182. doi:10.1016/j.algal.2013.01.010

Spoehr, H. A., & Milner, H. W. (1949). The chemical composition of *Chlorella;* effect of environmental conditions. *Plant Physiology* (Vol. 24). Stanford, California. doi:10.2307/4258176

Srivastava, A., & Prasad, R. (2000). Triglycerides-based diesel fuels. *Renewable & Sustainable Energy Reviews*, *4*(2), 111–133. doi:10.1016/S1364-0321(99)00013-1

Stephenson, A. L., Dennis, J. S., Howe, C. J., Scott, S. a, & Smith, A. G. (2010). Influence of nitrogen-limitation regime on the production by Chlorella vulgaris of lipids for biodiesel feedstocks. *Biofuels*, *1*(1), 47–58. doi:10.4155/bfs.09.1

Terigar, B. G., & Theegala, C. S. (2014). Investigating the interdependence between cell density, biomass productivity, and lipid productivity to maximize biofuel feedstock production from outdoor microalgal cultures. *Renewable Energy*, *64*, 238–243. doi:10.1016/j.renene.2013.11.010

Tonon, T., Harvey, D., Larson, T. R., & Graham, I. A. (2002). Long chain polyunsaturated fatty acid production and partitioning to triacylglycerols in four microalgae. *Phytochemistry*, *61*(1), 15–24. doi:http://dx.doi.org/10.1016/S0031-9422(02)00201-7

Tredici, M. R. (2010). Photobiology of microalgae mass cultures: understanding the tools for the next green revolution. *Biofuels*, *1*(1), 143–162. doi:10.4155/bfs.09.10

Vazhappilly, R., & Chen, F. (1998). Eicosapentaenoic acid and docosahexaenoic acid production potential of microalgae and their heterotrophic growth. *Journal of the American Oil Chemists' Society*, *75*(3), 393–397. doi:10.1007/s11746-998-0057-0

Vonshak, A., & Torzillo, G. (2004). Environmental Stress Physiology. In A. Richmond (Ed.), *Handbook of Microalgal Culture: Biotechnology and Applied Phycology* (pp. 57–82). Oxford; UK: Blackwell Science Ltd.

Warner, M. E., Lesser, M. P., & Ralph, P. J. (2010). Chlorophyll a Fluorescence in Aquatic Sciences: Methods and Applications. In J. D. Suggett, O. Prášil, & A. M. Borowitzka (Eds.), *Chlorophyll a Fluorescence in Aquatic Sciences: Methods and Applications, Developments in Applied Phycology 4* (pp. 209–222). Dordrecht: Springer Netherlands. doi:10.1007/978-90-481-9268-7

Wen, X., Geng, Y., & Li, Y. (2014). Enhanced lipid production in Chlorella pyrenoidosa by continuous culture. *Bioresource Technology*, *161*, 297–303. doi:10.1016/j.biortech.2014.03.077

Wieneke, K. (2015). Productivity of microalgal biomass constituents in simulated day night cycles: A model based approach, *31*(317).

Wijffels, R. H., & Barbosa, M. J. (2010). An outlook on microalgal biofuels. *Science (New York, N.Y.)*, *329*(5993), 796–799. doi:10.1126/science.1189003

Young, E., & Beardall, J. (2003). Photosynthetic function in *Dunaliella tertiolecta* (Chlorophyta) during a nitrogen starvation and recovery cycle. *Journal of Phycology*, *905*, 897–905. doi:10.1046/j.1529-8817.2003.03042.x

Appendix

Detailed model description

The mechanistic model by Breuer (2015) is predicting biomass growth and under continuous light. For the adaption towards outdoor light conditions, day/night- cycles and the biomass dark respiration were implemented in a previous work (Wieneke, 2015). A maximum light intensity of 1500 µmol/m²/s was assumed according to irradiance data of an average Dutch summer day. The sinus-shaped lightcurve is simplified to a 16 h long light period with a constant light intensity of 955 µmol/m²/s (Eq. 7).

$$\int_0^{16} 1500 \sin\left(\frac{2\pi}{2 * 16} x\right) dx = 15278.8 \qquad \text{Eq. 7}$$

Block-light for a light duration of 16 h:

$$\frac{15278.8}{16} = 954.93 \frac{\mu mol}{m^2 s} \qquad \text{Eq. 8}$$

Furthermore was a change in light intensities during the outdoor run introduced. The actual DLI[8] for each cultivation day was calculated and implemented as averaged light blocks during sunshine hours (as shown in Fig. 18).

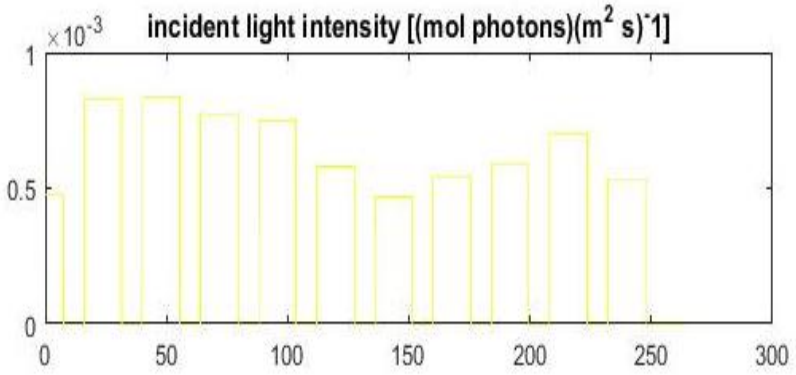

Figure 18: Light input for outdoor modelling, varying light intensities were implemented as block light with a varying DLI, based on actual measurements at the pilot site; cultivation period (x-axis) in hours

The model had yet to be validated for in- and outdoor production of *C. littorale* wildtype and S5. Hence further indoor experiments simulated outdoor summer conditions to compare the productivities for both strains.

[8] **DLI** (**D**aily **L**ight **I**ntegral), mol/m²/day, converted from PAR measurement station on site at AlgaePARC =PAR(average light intensity) (µmol/m^2/s)· h · 3600 / 1.000.000

Parameter estimations

Model parameters for all experiments can be seen in table 6 and were calculated based on experimental data (according to Breuer et al. 2015). Initial concentrations of TAG, STA, CHO, N, as well as the fractions of functional biomass XCHO, XSTAX, XCHOX, and X were directly obtained from experimental data.

Cellular nitrogen values were calculated based on the measured Q content (as described in 3.4) at the time point of inoculation and onset of nitrogen depletion. Q_{max} is representing the value at the highest biomass specific absorption cross section which is related to the maximum cellular nitrogen content. Q_{min} equals the minimum nitrogen content and Q_{deg} is taken from the time point of the highest starch concentration throughout the cultivation period (after which STA is converted to TAG).

Table 6: Overview of input parameters for the model simulations of Wt, S5 and outdoors experiments, units as applied in the model; confidence intervalls are indicated with ± for each value

Parameter	Unit	Description	Wildtype	S5	Outdoors
Constant parameters					
cd	s	duration of cultivation	240.5*3600	240*3600	264*3600
dds	s	duration of one day	24*3600	24*3600	/
dlds	s	duration of light per day	16*3600	16*3600	/
z	m	light path of the reactor	0.02	0.02	0.02
I0	$\frac{\text{mol}}{\text{m}^2 \cdot \text{s}}$	Incident light intensity	954.9 E-06	954.9E-07	/
Experimentally derived parameters					
Qmax	$\frac{\text{g N}}{\text{g DW}}$	cellular nitrogen content at maximum absorption cross section	0.0747 ± 0.015	0.0673 ± 0.018	0.0593 ± 0.008
Qmin	$\frac{\text{g N}}{\text{g DW}}$	minium cellular nitrogen content	0.0334 ± 0.015	0.0202 ± 0.013	0.0339 ± 0.014
Qdeg	$\frac{\text{g N}}{\text{g DW}}$	conc. of cellular N below which starch is converted to TAG	0.0334 ± 0.072	0.019 ± 0.006	0.0339 ± 0.001
rSTATAGmax	$\frac{\text{g TAG}}{\text{g DW} \cdot \text{s}}$	maximum interconversion rate of starch to TAG	1.77E-06 ±9.66E-07	2.20E-06 ±8.85E-07	6.485E-07 ±4.79E-08
rTAGXmax	$\frac{\text{g TAG}}{\text{g DW} \cdot \text{s}}$	maximum conversion rate of triacylglycerides to functional biomass	2.03E-07 ±1.79E-08	1.14E-07 ±2.09E-08	9.673E-07 ±3.07E-08
rSTAXmax	$\frac{\text{g TAG}}{\text{g DW} \cdot \text{s}}$	maximum conversion rate of starch to functional biomass	8.05E-07 ±5.83E-08	3.42E-07 ±6.98E-08	8.012E-07 ±4.57E-08
qphmaxrep		maximum photosynthetic rate at nitrogen replete conditions	9.11E-06 ±1.36E-06	9.99E-06 ±1.01E-06	7.675E-06 ±1.25E-06
XCHO	$\frac{\text{g CHO}}{\text{g DW}}$	carbohydrate fraction other than starch in biomass after nitrogen depletion	0.1402 ±0.062	0.1394 ±0.459	0.280 ±0.326
XSTAX	$\frac{\text{g STA}}{\text{g DW}}$	Fraction of starch in functional biomass	0.2463 ±0.097	0.1684 ±0.067	0.1995 ±0.085

XCHOX	$\frac{\text{g CHO}}{\text{g DW}}$	Fraction of carbohydrates other than starch in functional biomass	0.1004 ±0.032	0.0897 ±0.166	0.2197 ±0.159
arep	$\frac{\text{m}^2}{\text{g}}$	maximum absorption cross section under replete conditions	0.0877 ±0.008	0.0819 ±0.009	0.1012 ±0.009
X	$\frac{\text{g}}{\text{m}^3}$	initial concentration of functional biomass	459.97 ±19.66	484.32 ±17.612	433.6 ±16.754
TAG	$\frac{\text{g}}{\text{m}^3}$	initial concentration of triacylglyceride	1.6 ±0.36	18.1 ±2.49	2.81 ±0.05
STA	$\frac{\text{g}}{\text{m}^3}$	initial concentration of starch	132.4 ±5.63	172.1 ±23.93	68.29 ±3.43
CHO	$\frac{\text{g}}{\text{m}^3}$	initial concentration of carbohydrates other than starch	78.6 ±34.24	120.5 ±125.21	130.3 ±29.57
N	$\frac{\text{g (N in NO3)}}{\text{m}^3}$	initial amount of dissolved nitrate	124.1 ±2.08	126.16 ±3.04	114.4 ±1.99
pA	/	coefficient A for photon partitioning	0.0004 ±0.002	0.0014 ±0.004	0.0236 ±0.016
pB	/	coefficient B for photon partitioning	2.2053 ±1.004	1.7000 ±1.031	1.0802 ±0.903
Fitted parameters					
ms	$\frac{\text{mol photon}}{\text{g DW} \cdot \frac{Q}{Q_{max}} \cdot \text{s}}$	maintenance requirement per amount of reproducing biomass and time	1.80E-06	8.80E-07	6.25E-07
fpart	/	partition coefficient for replacing STA after nights in functionalbiomass	0.03	0.03	0.03

The maximum photosynthetic rate at nitrogen replete conditions (Eq. 9) is composed by the division of the maximal growth rate (during N-repletion) over the yield of biomass on photons (yXph).

$$q_{ph,max,rep} = \frac{\mu_{max}}{yXph} = \frac{\ln(cx_{t2} - cx_{t1})}{(t_2 - t_1) \cdot yXph} \quad \text{Eq. 9}$$

The maximum conversion rates $r_{TAG/X,max}$ (Eq. 10) and $r_{STA/X,max}$ (Eq.11) are expressing the highest degradation from starch and TAG respectively to functional biomass.

$$r_{TAG/X,max} = \frac{XTAG_{t1} - XTAG_{t2}}{t_2 - t_1} \quad \text{Eq. 10}$$

$$r_{STA/X,max} = \frac{XSTA_{t1} - XSTA_{t2}}{t_2 - t_1} \quad \text{Eq. 11}$$

The maximum conversion rate from starch to TAG is directly derived from experimental data and only possible under nitrogen deplete conditions and Q lower than Q_{deg} (Eq. 12).

$$r_{STA/TAG,max} = \frac{XSTA_{t1} - XSTA_{t2}}{t_2 - t_1} \quad \text{Eq. 12}$$

The partition coefficient f_{TAG} (Eq. 13) is defined as the ratio of photons used for the production of TAG to the amount of photons used for the production of starch. For the parameter estimation, the amount of generated STA (ΔSTA) is transformed to the amount of TAG, that could have been produced instead, using the yields of STA and TAG on photons (ySTAph and yTAGph).

$$f_{TAG} = \frac{\text{photons for TAG synthesis}}{\text{photons for starch synthesis}} = \frac{\Delta TAG}{\Delta TAG + \frac{\Delta STA \cdot yTAGph}{ySTAph}} \qquad \text{Eq. 13}$$

The proportion between TAG and starch synthesis is specific for each scenario and defined through the estimated parameters pA and pB. Through the corellation of the partition coefficient f_{TAG} to Q (cellular nitrogen content) it is becoming a function of time. It is describing the carbon partitioning towards STA and TAG, which biological mechansims is not fully understood.

$$f_{TAG} = \min \begin{Bmatrix} pA \cdot Q^{-pB} \\ 1 \end{Bmatrix} \qquad \text{Eq. 14}$$

The parameter a_{rep} (Eq. 15) defines the maximum absorption cross section of nitrogen replete biomass. This factor is dependent on the species and state of photoacclimatisation of the algae (Macintyre, Kana, Anning, & Geider, 2002). Light scattering was considered by a subtraction of the average absorption (abs_λ) between 740 nm and 750 nm.

$$a_{rep} = \frac{\sum_{400}^{700} abs_\lambda \frac{\ln(10)}{z}}{300 \cdot c_{DW}} \qquad \text{Eq. 15}$$

with z: light path of the precision cell

c_{DW}: dry weight concentration in the cell

Fitted parameters

The maintenance requirements (m_s) for both the wildtype (in- and outdoor cultivation) and S5 was estimated in Matlab by fitting the model dependend on the biomass concentration and evaluation of the resulting square errors (maximal R-square).

$$R^2 = 1 - \frac{SSE}{SST} = 1 - \sum_t \left(\frac{c_x(t) - modelc_x(t)}{c_x(t) - cx_{avg}} \right)^2 \qquad \text{Eq. 16}$$

Ms was calculated for each experiment individually due to the differing cultivation modes and conditions. The estimated maintenance requirements were all higher than in previous experiments, though remaining in the same magnitude.

The parameter f_{part} is partitioning the energy towards the replacement of (during night) degraded starch. It was estimated in a previous experiment (Wieneke, 2015) by fitting the model to the maximized R-square, and is assumed to be constant for the experiments at hand.

At the time point where all starch in functional biomass is restored, the available energy is partitioned normally (as under continuous conditions) again and f_{part} is set to zero (Eq. 17).

$$f_{part} = \begin{cases} f_{part} & \text{if } degSTA < 0 \\ 0 & \text{if } degSTA = 0 \end{cases} \quad \text{Eq. 17}$$

Theoretical yields

The values for the maximum photosynthetic yields (yXph, yCHOph, ySTAph and yTAGph) in a green algae are taken from Kliphuis et al. (2012) and were experimentally derived by experiments with *Chlamydomonas reinhardtii*. Due to the adaption of the model to day/night- cycles (and therefore night respiration) a set of conversion yields (yXTAG, yXSTA, yATPph, yATPSTA) was established by Wieneke 2015 based on metabolic pathways.

Table 7: Theoretical maximum photosynthetic yields and conversion yields used in the model estimations

Parameter	Unit	Value	Description
yXph	$\frac{g\ X}{mol\ photon}$	1.62	yield of functional biomass on photons when grown on NO3-
yCHOph	$\frac{g\ CHO}{mol\ photon}$	3.24	yield of other carbohydrates than starch on photons
ySTAph	$\frac{g\ STA}{mol\ photon}$	3.24	yield of Starch on photons
yTAGph	$\frac{g\ TAG}{mol\ photon}$	1.33	yield of triacylglycerides on photons
yTAGSTA	$\frac{g\ TAG}{g\ STA}$	0.39	yield of triacylglycerides on starch
yXCHO	$\frac{g\ X}{g\ CHO}$	0.644	conversion yield of functional biomass on other carbohydrates
yXSTA	$\frac{g\ X}{g\ STA}$	0.644	conversion yield of functional biomass on starch
yXTAG	$\frac{g\ X}{g\ TAG}$	1.404	conversion yield of functional biomass on triacylglycerides
yATPSTA	$\frac{mol\ ATP}{g\ STA}$	0.149	yield of ATP on starch
yATPTAG	$\frac{mol\ ATP}{g\ TAG}$	0.325	yield of ATP on TAG
yATPph	$\frac{mol\ ATP}{mol\ photons}$	0.375	yield of ATP on photons

Model extension for simulated day night cycles

As Breuer et al., 2015 was developing the model for cultivation of algae on continuous light, a model extension for the work with *C. littorale* in simulated outdoor conditions had to be made. In the following the implemented change of functions for a previous work (Wieneke, 2015) can be seen.

Equation 18 is introducing a light change during the cultivation day by using a step function. The light intensity (I0) is only applied during the daylight hours per day (dlds), leaving a dark period for the rest of the day (I=0). Further parameters: t (cultivation time), nd (number of day), dds (duration of day).

$$I(t) = \begin{cases} I_0 & \text{if } (t - nd \cdot dds) < dlds \\ 0 & \text{if } (t - nd \cdot dds) \geq dlds \end{cases} \quad \text{Eq.18}$$

In addition to the regulation of the timepoint for lightning in Eq. 18, a function for the light distribution within the reactor was implemented in Eq. 19. The light scenario within the reactor is incorporating the constant light intensity (I0) and the attenuation model of Lambert-Beer (whereas the attenuation coefficient (a) equals the absorption cross section (a)). All light scattering was neglected.

$$I(z) = I_0 \cdot e^{-a \cdot c_x \cdot z} \quad \text{Eq. 19}$$

with z: light path
c_x: total biomass concentration

Metabolic principles that are accountable for the partitioning of available energy are under a strong influence of the progress of nitrogen depletion. Through the cellular nitrogen content (Q) those effects can be surrogated in a simplified way.

Since the composition of functional biomass is not constant anymore due to dark respiration, a new equation for the cellular nitrogen content (Q) had to be found (Eq. 20). The amount of degraded starch over night (degSTA) is taking into consideration (substracted) for the correct concentration of functional biomass (X).

$$Q = Q_{max} \cdot \frac{X - degSTA}{c_x} \quad \text{Eq. 20}$$

The quantum yield (QY, Eq. 21) is expressing the available fraction of absorbed photons that is not dissipated as heat. A correction of the quantum yield (QY) is subsequently with the previous equation. As the cellular nitrogen content may exceed Q_{max} due to starch degradation during nights, the quantum yield (QY) is overestimated during nights. Therefore Equation 6 assures a maximum QY of 1, avoiding the utilization of more energy than available.

$$QY = \min\left\{\begin{matrix}\left(1-\frac{Q_{min}}{Q}\right)\cdot\left(1-\frac{Q_{min}}{Q_{max}}\right)^{-1} \\ 1\end{matrix}\right\} \quad \text{Eq. 21}$$

The available energy is partitioned to the *de novo* synthesis of biomass constituents with respect to differing yields for TAG, STA, CHO and reproducing biomass estimated, which have been analyzed through flux balance analyzes. Breuer et al. described the conversion of STA to TAG. As a model extension, yields and reaction rates for the conversion of STA and TAG to reproducing biomass were included allowing non-reproducing biomass being present as initial model input.

The following equations (Eq 22. - Eq. 28) describe the specific production rates for any biomass constituents during the light period based on the average biomass specific photosynthetic rate ($q_{ph,avg}$). All specific production rates (Eq. 22-28) are depending on the available energy from photosynthesis. Metabolic principles that are accountable for the partitioning of available energy are under a strong influence of the progress of nitrogen depletion. Maintenance requirements are biomass specific and through the factor of cellular nitrogen content (Q) only depending on the fraction of functional biomass.

One of the main important points of (the model) of a nitrogen-runout batch is the regulation of mechanisms for the switch between N-deplete and N-replete phase. As long as dissolved nitrogen (N, as nitrate) is available, functional biomass is synthesized exclusively.

Eq. 22 is showing the specific production rate of reproducing biomass and is extended (from the continuous light functions) with the correction of starch degradation during night, leaving the same composition before and after the night. The fraction f_{part} is adjusting the available energy during the day due to the replacement of starch in the functional biomass after night respiration. Also included is the conversion of TAG to functional biomass ($r_{TAG/X} \cdot$ yXTAG). No functional biomass can be produced when the dissolved nitrogen concentration is zero.

$$qX = \begin{cases} \overbrace{yXph \cdot \left(q_{ph,avg} - \frac{m_s \cdot Q}{Q_{max}}\right) \cdot (1 - f_{part}) + r_{TAG/X} \cdot yXTAG + STAinXdeg}^{qX1} & \text{if } N > 0 \text{ and} q_{ph,avg} > \frac{m_s \cdot Q}{Q_{max}} \\ STAinXdeg & \text{if } N = 0 \text{ and } q_{ph,avg} > \frac{m_s \cdot Q}{Q_{max}} \end{cases} \quad \text{Eq. 22}$$

$$\text{with } STAinXdeg = ySTAph \cdot \left(q_{ph,avg} - \frac{m_s \cdot Q}{Q_{max}}\right) \cdot f_{part}$$

The remaining production rates (Eq. 23: carbohydrates, Eq. 24: starch, Eq. 25: TAGs) are corresponding to the original model, with the exception of a correction of degraded starch in the total carbohydrates (Eq. 23).

Under nitrogen depletion firstly the general carbohydrate (other than starch) levels are kept constant. Expressed through the multiplication of available energy and the production yield of CHO on photons ($yCHO_{ph}$). As the carbohydrate levels in functional biomass are attempted to kept stable, CHO is only produced in case of a lower CHO content than the average in functional biomass ($xCHO \leq XCHO$).

$$qCHO = \begin{cases} \left(\left(q_{ph,avg} - \frac{m_s \cdot Q}{Q_{max}}\right) \cdot (1 - f_{part}) - \frac{qX1}{yXph}\right) \cdot yCHOph & \text{if } xCHO \leq XCHO \\ 0 & \text{if } xCHO > XCHO \end{cases} \quad \text{Eq. 23}$$

$$\text{with } xCHO = \frac{XCHOX \cdot (X - degSTA) + CHO}{c_x}$$

The residual energy after CHO synthesis is partitioned between TAG and starch (yields on photons see Tab. 7). For both cases the available energy for synthesis is constructed out of the specific photosynthetic energy (corrected for maintenance energy), the leftover energy after replacing CHO into functional biomass after nights and the energy already consumed for X and CHO synthesis.

The proportion between TAG and starch synthesis is specific for each scenario and defined through f_{TAG}, which is the energy portion used for TAG synthesis and primarily depending on the cellular nitrogen content. Respectively, $(1\text{-}f_{TAG})$ is the surplus energy going into starch production. In addition to the particular yields on photons, the conversion from starch to TAG (only below Qdeg, Eq. X) is included. Finally the conversiono rates of TAG and STA into functional biomass are completing the functions.

$$qTAG = \left\{ \begin{array}{r} \left(\left(q_{ph,avg} - \frac{m_s \cdot Q}{Q_{max}} \right) \cdot \left(1 - f_{part} \right) - \frac{qX1}{yXph} - \frac{qCHO}{yCHOph} \right) \cdot f_{TAG} \cdot yTAGph \\ + r_{STA/TAG} \cdot yTAGSTA - r_{TAG/X} \end{array} \right\} \quad \text{Eq. 24}$$

$$qSTA = \left\{ \begin{array}{r} \left(\left(q_{ph,avg} - \frac{m_s \cdot Q}{Q_{max}} \right) \cdot \left(1 - f_{part} \right) - \frac{qX1}{yXph} - \frac{qCHO}{yCHOph} \right) \cdot \left(1 - f_{TAG} \right) \cdot ySTAph \\ - r_{STA/TAG} - r_{STA/X} \end{array} \right\} \quad \text{Eq.25}$$

The specific nitrogen consumption rate had to be redefined as the night biomass loss (occurring under day/night cycles) would increase the dissolved nitrogen concentration (which is not the case). Equation 26 is implementing the replacement of starch into functional biomass (STAinXdeg) and avoiding thereby a rising dissolved nitrogen level.

$$qN = \left\{ \begin{array}{ll} -(qX - STAinXdeg) \cdot Q_{max} & \text{if } qX \geq 0 \\ r_{TAG/X} \cdot yXTAG & \text{if } qX < 0 \end{array} \right\} \quad \text{Eq. 26}$$

With the shift to a cultivation with day/night cycles, metabolic mechanisms during the dark phase had to be considered. No photosynthetic energy is available (removed energy supply and ms), thus no synthesis of biomass constituents is taking place. Rather would the dark respiration cause a night biomass loss and degrade energy storing components (starch) to cover the maintenance requirements. Equations 27 and 28 are restricted to the dark phase (through $q_{ph,avg}$), while during the lightperiod Eq. 22 and Eq. 25 apply.

The maintenance energy during night is preferably cover by accumulated starch (STA), if there is none available, starch will be degraded out of the functional biomass (STAinXdeg). The rate of reproducing biomass in the night (Eq. 27) is therefore implemented by the conversion factor of starch to functional biomass (rSTA/X).

$$qX = \left\{ \begin{array}{ll} r_{STA/X} \cdot yXSTA + r_{TAG/X} \cdot yXTAG & \text{if } STA > 0 \text{ and } q_{ph,avg} < \frac{m_s \cdot Q}{Q_{max}} \\ r_{TAG/X} \cdot yXTAG + STAinXdeg & \text{if } STA = 0 \text{ and } q_{ph,avg} < \frac{m_s \cdot Q}{Q_{max}} \end{array} \right\} \quad \text{Eq. 27}$$

$$\text{with } STAinXdeg = -\frac{m_s \cdot Q}{Q_{max}} \cdot \frac{yATPph}{yATPSTA}$$

Equation 28 uses a decrease of the biomass specific production rate of starch ($r_{STA/X}$) for starch degradation (covering ms).

$$qSTA = \begin{cases} -r_{STA/TAG} - r_{STA/X} - \frac{m_s \cdot Q}{Q_{max}} \cdot \frac{yATPph}{yATPSTA} & \text{if } STA > 0 \text{ and } q_{ph,avg} < \frac{m_s \cdot Q}{Q_{max}} \\ 0 & \text{if } STA = 0 \text{ and } q_{ph,avg} < \frac{m_s \cdot Q}{Q_{max}} \end{cases} \quad \text{Eq. 28}$$

The general production rate for total biomass Eq. 29 was applied unchanged from the original model (Breuer et al., 2015).

$$c_x = X + TAG + STA + CHO \quad \text{Eq. 29}$$

Total biomass cx is the total amount of functional biomass, TAG, starch and CHO. Proteins, ash and other components that are not already included in the functional biomass are neglected.

Available energy from photosynthesis

All specific production rates (Eq. 22-28) are depending on the available energy from photosynthesis. The average biomass specific photosynthetic rate ($q_{ph,avg}$, Eq. 30) is using a photosynthesis-irradiance response curve (with a hyperbolic tangent function by (JASSBY and PLATT 1976, following the attenuation model of Lambert-Beer) to describe the light distribution within the reactor. This factor is multiplied with the integrated maximum photosynthetic rate ($q_{ph,max}$, Eq. 9) over the light path (z). Light scattering is neglected and the light is assumed to be perpendicular.

$$q_{ph,avg} = \frac{1}{z} \int_0^z q_{ph,max} \cdot \tanh\left(\frac{a \cdot QY \cdot I_0 \cdot e^{-a \cdot c_x \cdot z}}{q_{ph,max}}\right) \quad \text{Eq.30}$$

with z: light path
c_x: total biomass concentration

The absorption cross section (a, Eq. 31) is definied as a correlation between the maximum absorption cross section (of nitrogen replete biomass, Eq. 15) and the cellular nitrogen content (Q). Pigments are a constant fraction of reproducing biomass and, thus, diluted over the biomass, when other constituents than reproducing biomass are generated.

$$a = a_{rep} \cdot \frac{Q}{Q_{max}} \quad \text{Eq. 31}$$

The conversion of starch and TAG to functional biomass (Eq. 32 and Eq. 33) can only take place under nitrogen replete conditions as nitrogen is required for N-containing compounds in functional biomass (genetic material, proteins etc.).

$$r_{STA/X} = \begin{cases} r_{STA/X,max} & \text{if } N > 0 \text{ and } STA > 0 \\ 0 & \text{if } N < 0 \text{ or } STA = 0 \end{cases} \quad \text{Eq. 32}$$

$$r_{TAG/X} = \begin{cases} r_{TAG/X,max} & \text{if } N > 0 \text{ and } TAG > 0 \\ 0 & \text{if } N < 0 \text{ or } TAG = 0 \end{cases} \quad \text{Eq. 33}$$

In case the cellular nitrogen level Q_{deg} is reaching lower levels than Q_{min}, a degradation of starch to TAG with the rate of $r_{STA/TAG,max}$ can take place (Eq. 34).

$$r_{STA/TAG} = \begin{cases} r_{STA/TAG,max} & \text{if } Q \leq Q_{deg} \text{ and } STA > 0 \\ 0 & \text{if } Q > Q_{deg} \text{ and } STA = 0 \end{cases} \quad \text{Eq. 34}$$

Relative spectral emission for Infors 5 LED-panel

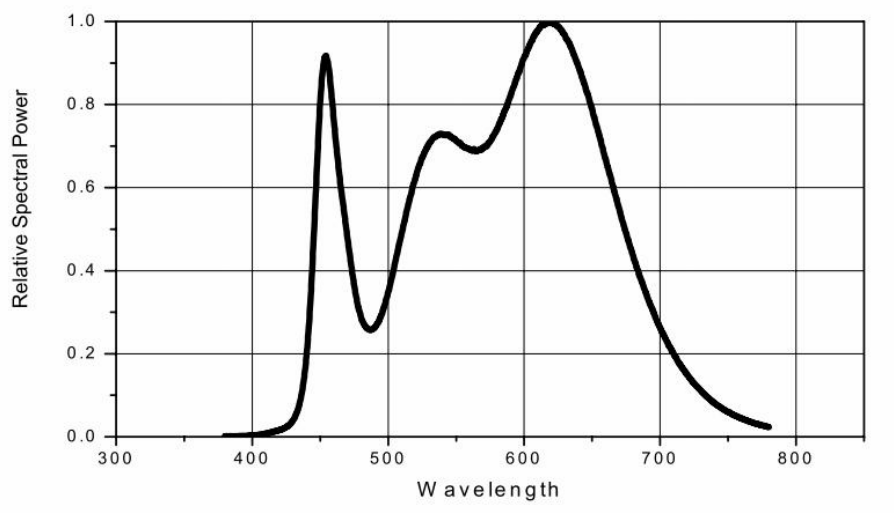

Figure 19: Spectral distribution of the "warm white" high power LED panel used for the indoor experiments of Wt and S5 in the Infors 5 flat panel PBR

Confidence intervals of model parameters

As described in 3.6, 95 % confidence intervals were calculated to evaluate the fit between measured data and model simulations of Wt, S5 and outdoor experiments. CIs of total biomass (Fig. 20), TAGs (Fig. 21) and starch (Fig. 22) are shown.

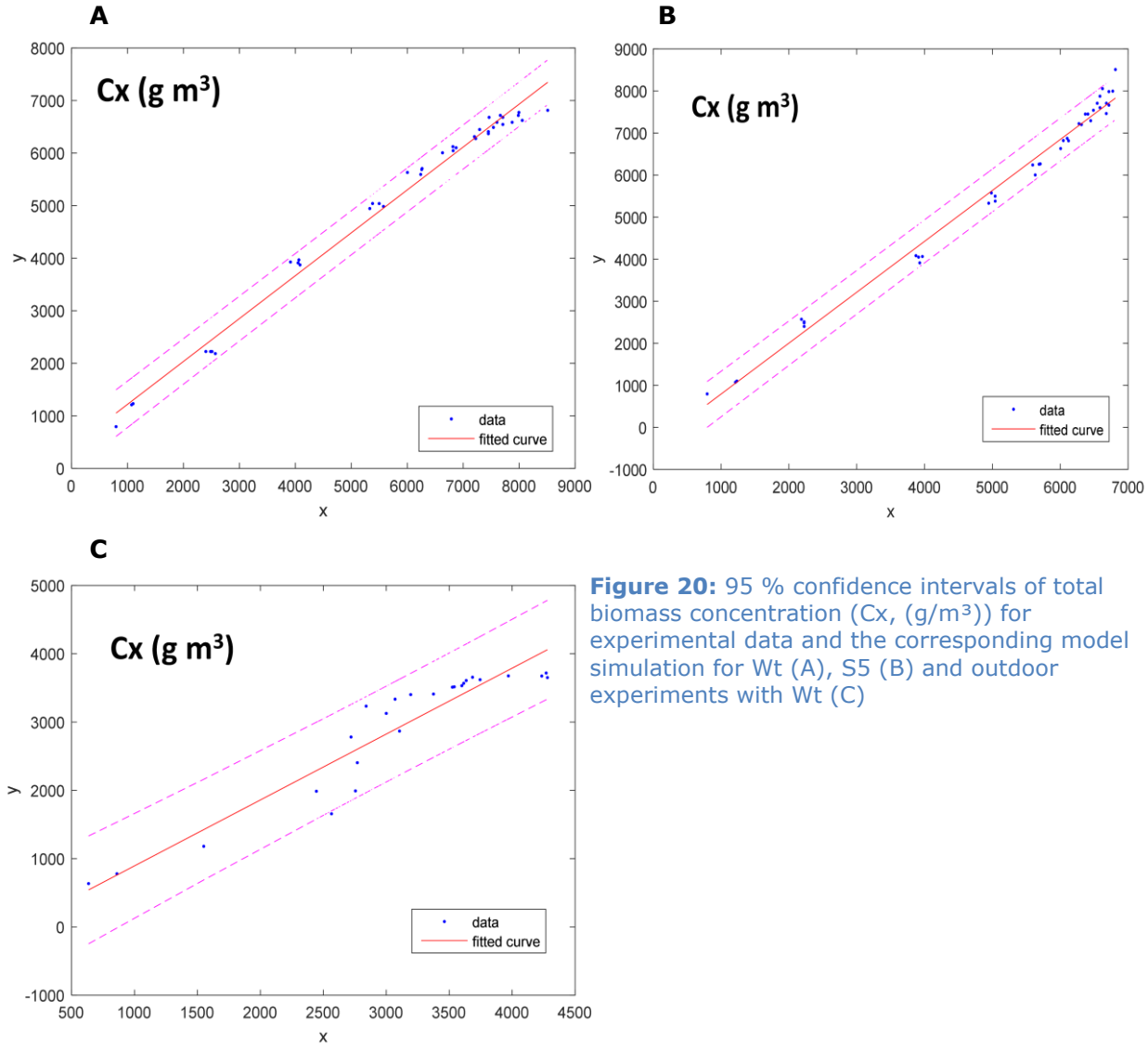

Figure 20: 95 % confidence intervals of total biomass concentration (Cx, (g/m³)) for experimental data and the corresponding model simulation for Wt (A), S5 (B) and outdoor experiments with Wt (C)

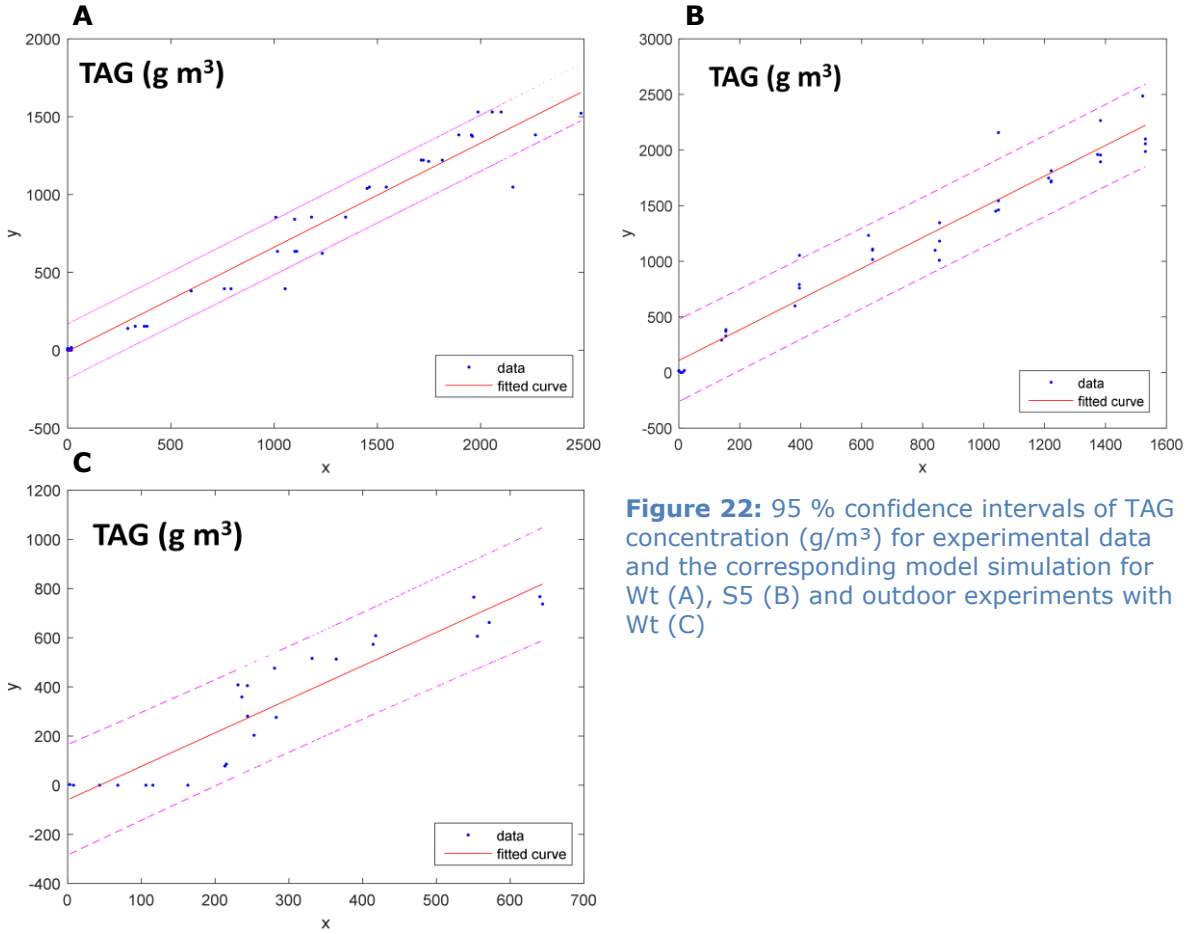

Figure 22: 95 % confidence intervals of TAG concentration (g/m³) for experimental data and the corresponding model simulation for Wt (A), S5 (B) and outdoor experiments with Wt (C)

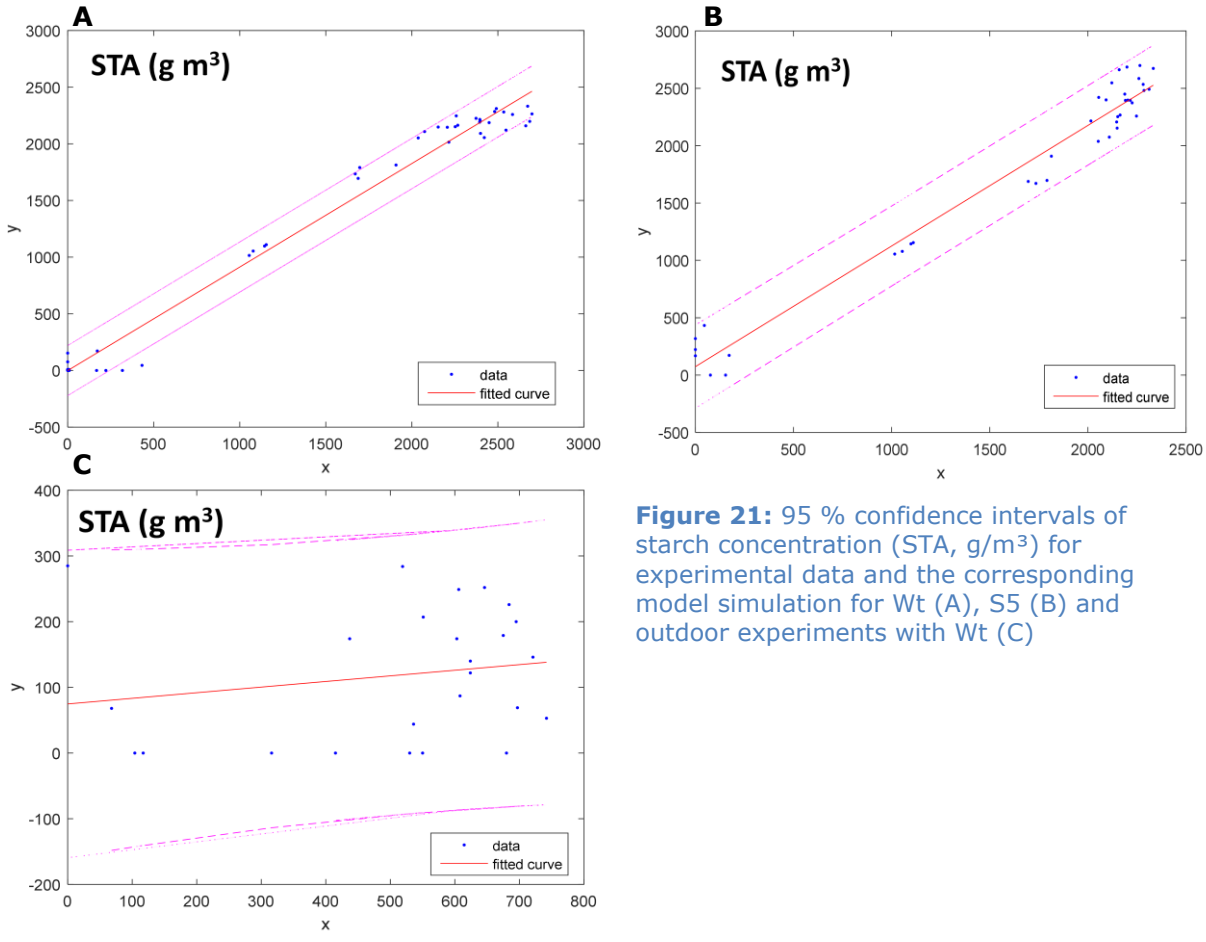

Figure 21: 95 % confidence intervals of starch concentration (STA, g/m³) for experimental data and the corresponding model simulation for Wt (A), S5 (B) and outdoor experiments with Wt (C)